3-6-2004

Systems-Level Feasibility Analysis of a Microsatellite Rendezvous with Non-Cooperative Targets

Allen R. Toso

SYSTEMS-LEVEL FEASIBILITY ANALYSIS OF A MICROSATELLITE RENDEZVOUS WITH NON-COOPERATIVE TARGETS

THESIS

Allen R. Toso, Major, USAF

AFIT/GSS/ENY/04-M06

DEPARTMENT OF THE AIR FORCE
AIR UNIVERSITY

AIR FORCE INSTITUTE OF TECHNOLOGY

Wright-Patterson Air Force Base, Ohio

The views expressed in this thesis are those of the author and do not reflect the official policy or position of the United States Air Force, Department of Defense, or the U.S. Government.

AFIT/GSS/ENY/04-M06

SYSTEMS-LEVEL FEASIBILITY ANALYSIS OF A MICROSATELLITE RENDEZVOUS WITH NON-COOPERATIVE TARGETS

THESIS

Presented to the Faculty

Department of Aeronautics and Astronautics

Graduate School of Engineering and Management

Air Force Institute of Technology

Air University

Air Education and Training Command

In Partial Fulfillment of the Requirements for the

Degree of Master of Science (Space Systems)

Allen R. Toso

Major, USAF

March 2004

AFIT/GSS/ENY/04-M06

SYSTEMS-LEVEL FEASIBILITY ANALYSIS OF A MICROSATELLITE RENDEZVOUS WITH NON-COOPERATIVE TARGETS

Allen R. Toso

Major, USAF

Approved:

//signed//	6 Mar 04
Dr Steven G. Tragesser (Chairman)	Date
//signed//	6 Mar 04
Richard G. Cobb, Major, USAF (Member)	Date
//signed//	5 Mar 04
Joerg D. Walter, Major, USAF (Member)	Date

AFIT/GSS/ENY/04-M06

Abstract

The United States is very dependant upon the use of space. Any threat to our ability to use it as desired deserves significant study. One such asymmetric threat is through the use of a microsatellite. The feasibility of using a microsatellite to accomplish an orbital rendezvous with a non-cooperative target is being evaluated. This study focused on identifying and further exploring the technical challenges involved in achieving a non-cooperative rendezvous.

A systems engineering analysis and review of past research quickly led to a concentration on the guidance, navigation, and control (GN&C) elements of the microsatellite operation. While both the control laws and orbit determination have been previously evaluated as feasible, the integration of the two remained in question. This research first validated past efforts prior to exploring the integration. Impulsive and continuous thrust control methods, and linear and nonlinear estimator filters were all candidate components to a potential system solution.

A simple yet robust solution could not be found to meet reasonable rendezvous criteria, using essentially off-the-shelf technology and algorithms. Results reveal a simple linear filter is a misapplication and will not at all work. A nonlinear filter coupled with either a continuous or impulsive thrust controller was found to get somewhat close, but never close enough to attach to the target satellite. Successful GN&C subsystem

integration could only be achieved for a very simple case ignoring orbit perturbations such as the earth's oblateness. A top-level system architecture for a non-cooperative rendezvous microsatellite has been developed. The technical complexity, however, requires more complex algorithms to solve the rendezvous problem.

Acknowledgments

I would like to thank my advisor, Dr. Steven Tragesser, for his insightful guidance throughout this learning endeavor. The growth I have experienced is due, in large part, to his persistent efforts challenging me to work outside my comfort zone. Dr. Tragesser has passed to me a much greater appreciation for the technical challenges involved in space systems development and evaluation.

I would also like to thank all students of ENY-04M for their personal and professional relations. I owe a special thanks to my fellow Space Systems and Astronautical Engineering comrades for their encouragement and wisdom. Maj John Seo also deserves acknowledgment for his critical analysis and friendship.

Finally, I am deeply indebted to my wonderful wife who provided both the necessary motivation and support required to complete all aspects of this project.

Allen R. Toso

Table of Contents

Page

Page

List of Figures

Page

Page

Page

List of Tables

Page

SYSTEMS-LEVEL FEASIBILITY ANALYSIS OF A MICROSATELLITE RENDEZVOUS WITH NON-COOPERATIVE TARGETS

I. Introduction

Background

> We are entering, or perhaps have already entered, an era in which the use of space will exert such profound influence on human affairs that no nation will be fully able to control its own destiny without significant space capabilities.
>
> –General Robert T. Herres (USAF)
> Vice Chairman of the JCS, 1988

Although the quote above may seem a bit dated, we are just now beginning to fully understand the ramifications of such statements. The United States has for some time led the world in the use of space-based resources for military as well as civilian operations. Our large competitive advantage is now being challenged, however. Gen Lance Lord, Commander of Air Force Space Command (AFSPC) discussed this issue with space industry leaders in November 2003. The General stated that, "Our adversaries – and even future adversaries – know the value we place on space to enhance, improve and transform all our operations. They will increasingly try to deny us the asymmetric advantage that space provides" (Wilson, 2004).

As the potential benefits of space operations are more broadly understood, more capabilities are being transferred to the ultimate high ground. In an interview last October with *Inside the Pentagon*, Lt Gen Dan Leaf, Vice Commander of AFSPC,

described just how dependent the United States is on our space assets. He chose to depict our space capabilities as "woven inextricably through our overall military capabilities" (Grossman, 2003a). We have indeed moved much beyond the first space war of Desert Storm in 1991 when GPS, DSP, and exclusive national systems were used to support only selected air and ground operations.

Given our critical dependence upon and potential threat to our space assets, any focused research in this arena may prove valuable to space policy makers, developers and operators alike. Gen Lord declared that, "It is our duty to preserve, protect and defend the high ground of space and we must have the ways and means of detecting, characterizing, reporting and responding to attacks in the medium of space" (Wilson, 2004). This research effort is aimed at contributing to characterizing a specific potential space threat.

Space Control

The concept of space control involves both offensive and defensive activities to ensure a desired level of advantage. From the very indiscriminate nuclear systems to the laser-focused Star Wars initiative, history provides a colorful review of space control attempts. Only one select example will be quickly discussed here. Current space control doctrine will be presented next. Finally, the above will be used to put this research into the larger context of current Air Force counterspace activities. This, in itself, is a systems engineering activity as a key step in the evaluation of any potential system is to view both internal and external environments.

Traditionally, an Anti-Satellite (ASAT) system has been viewed as having the purpose of negating the functional mission of the target space asset. This can be accomplished by various methods. Directing energy on the satellite from a ground or space-based illuminating device; placing co-orbiting "mines" in space adjacent to the target; direct ascent; achieving a co-orbit with the target satellite and "catching up" to it; and launching a device from a high-altitude aircraft have all been attempted (Johnson-Freese, 2000).

The United States has undergone the most extensive ASAT development activity. Project SAINT (SAtellite INTerceptor) began in the late 1950's. The program extensively covered a wide range of technologies for interception, inspection, and destruction of enemy spacecraft (SAINT, 2003). The Concept of Operations, or CONOPS, entailed rendezvous with a target satellite, inspection with television cameras, and then disabling it somehow. Project SAINT was restructured several times and eventually canceled in 1962 before reaching operational status.

The doctrine of Space Control has only recently emerged within both the DoD and the Air Force. DoD 3100.10 defines Space Control as: "Combat and combat support operations to ensure freedom of action in space for the United States and its allies and, when directed, deny an adversary freedom of action in space." It further delineates Space Control mission areas to include surveillance of space; protection of U.S. and friendly space systems; prevention of an adversary's ability to use space systems and services for purposes hostile to U.S. national security interests; negation of space systems and

services used for purposes hostile to U.S. national security interests; and directly supporting battle management, command, control, communications, and intelligence.

The Air Force uses Air Force Doctrine Document (AFDD) 2-2, "Space Operations," to specify the approved methods and means of conducting counterspace activities. The function of Counterspace is assigned to fulfill the Space Control mission area. AFDD 2-2 describes Counterspace Operations consisting of those operations conducted to attain and maintain a desired degree of space superiority by allowing friendly forces to exploit space capabilities while negating an adversary's ability to do the same.

As with most functional areas, Counterspace is divided into offensive and defensive components. Offensive Counterspace (OCS) operations preclude an adversary from exploiting space to his advantage (AFDD 2-2, 2001). The usual continuum of Deception, Disruption, Denial, Degradation, and Destruction are available means.

Defensive Counterspace (DCS) operations preserve U.S./allied ability to exploit space to its advantage via active and passive actions to protect friendly space-related capabilities from enemy attack or interference (AFDD 2-2, 2001). Both active (e.g. detect, track, and identify) and passive (e.g. survivability) techniques are promoted. Space Control cannot be effectively achieved without both robust OCS and DCS capabilities.

This research directly supports the ability to conduct DCS operations. Analyzing the technical challenges arising from a microsatellite rendezvous concept helps characterize feasible adversary OCS capabilities, and thus necessary U.S. defenses. Lt

Gen Leaf recently discussed a future space activity identification capability gap resulting from a multi-service review. The general asserted,

> We must have good, timely space situational [SA] awareness – not just because of our increased reliance on space capability and the complexity of all that occurs in space, but also because of potential threats to those capabilities. The number of nations that utilize space-based capabilities and the way that they are used are both expanding. So we have to ensure that our space SA…doesn't simply track objects but is able, in a timely manner, to recognize changing situations in space, just as we do in the atmosphere or in the sea. (Grossman, 2003b)

This theoretical capability gap, between what we need and what we have, is not well understood. The fact that we do not have a good characterization of feasible adversary OCS capabilities leads to a poor understanding of the gap. Better comprehension of this potential threat is the aim of this study.

Problem Statement/Research Objectives

The overall objective of this research effort is the analysis of potential counterspace threats from foreign countries or organizations. Counterspace operations that are possible with readily available technology and information will be evaluated. This effort is a systems design study on a potential foreign offensive counterspace satellite to identify the technical challenges arising from rendezvous with a non-cooperative satellite.

The specific objective is to determine if it is possible to design, build, and operate an offensive microsatellite using off-the-shelf technology and information that is publicly available. The microsatellite must be able to maneuver to rendezvous with a target satellite, maintain proximity with the target, and perform its mission.

For this project, it is assumed the microsatellite will be placed into an orbit similar to that of the target satellite, approximately 1000 km behind it in the same orbital plane. The microsatellite then performs rendezvous maneuvers to approach the target.

It is further assumed the microsatellite has perfect knowledge of its own position and velocity but must estimate that of the target. The microsatellite would likely begin with an orbit solution derived from off-board sensors. As the microsatellite approaches the target, on-board sensors would detect the target satellite and an updated orbit solution would be calculated. This would allow the microsatellite to complete the rendezvous without any feedback from the target satellite.

The unique aspect of this problem involves the use of an integrated estimator and controller to more closely model reality. This research then takes an additional step to make a systems-level feasibility assessment of the proposed microsatellite threat.

Methodology

A high-level systems view was coupled with a more detailed technical assessment to form the approach to answer the research objective. Systems engineering design tools were first used to identify the driving technical areas to focus on. Once identified, these guidance, navigation & control (GN&C) algorithms were studied extensively to appreciate the evident as well as subtle application challenges involved. Finally, the systems view was again taken to make the concluding feasibility assessment.

II. Literature Review

Chapter Overview

The purpose of this chapter is to provide a review of microsatellite technology and recent rendezvous-related research efforts. Applicable industry, academic and military microsatellite efforts are presented. Significant challenges regarding GN&C are highlighted.

Previous microsatellite rendezvous research results are reviewed next. The focus is on AFIT work leading up to this research, and supplemented were appropriate. The control laws and orbit determination/navigation required to support a non-cooperative rendezvous make up the primary body of research drawn upon in developing the starting point for this project.

Literature reviewed was primarily limited to open-source as the feasibility of a relatively low-tech solution using off-the-shelf technology and publicly available information is being evaluated. The review highlights several key findings as summarized below. The microsatellite industry is rapidly becoming capable of providing system solutions to a very diverse set of problems, to include space control applications. Rendezvous with a non-cooperative target is a non-trivial operation, but key elements of control and orbit determination have been separately demonstrated. Little research has been accomplished to evaluate systems-level feasibility from a systems engineering perspective.

Microsatellites

A microsatellite is a small satellite generally considered to have mass less than 100 kg. They are typically more economical to develop and operate, and quicker from concept to operation compared to traditional satellites. There has been considerable effort in the research and development of capabilities using microsatellites of late. Common uses include visible sensing, multi-spectral imaging, radar, infrared, communications, and navigation.

Surrey Satellite Technology Ltd. (SSTL) is a world leader in the development of microsatellite technologies. Since SSTL spun off from the University of Surrey Engineering Department in 1985, they have launched roughly one spacecraft per year, pushing small satellite technology (Morring, 2003). SSTL claims they were the first professional organization to offer low-cost small satellites with rapid response employing advanced terrestrial technologies. They indeed have an impressive track record in an emergent field.

SSTL's AISAT-1, developed for the international Disaster Monitoring Constellation, has successfully completed over one year of operations. Imagery derived has been useful to authorities with areas of responsibility from hydrological mapping to the threat of locust plagues. The AISAT-1 microsatellite is pictured in Figure 1 below.

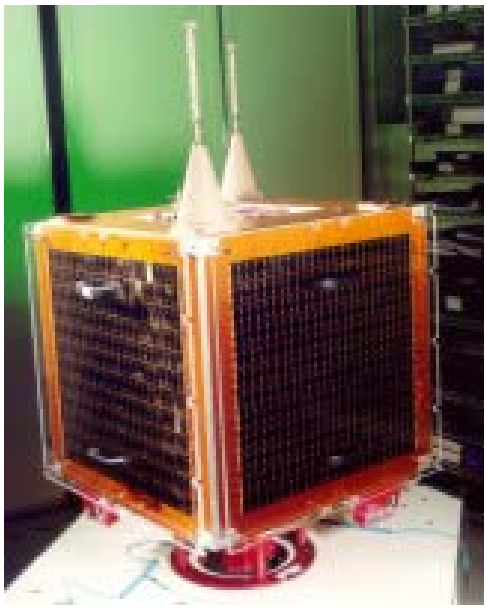

Figure 1. AISAT-1 Microsatellite (SSTL, 2003)

The European Space Agency (ESA) is also a significant player using small satellites for advanced science missions. ESA's Project for On-board Autonomy (Proba) is using a microsatellite to flight test on-orbit operational autonomy. Proba-1, launched in October 2001, returned high-resolution images of Earth and conducted various radiation studies (Morring, 2003). Proba-2, scheduled for launch in 2006, will study the sun, providing early warnings of solar flares. Frederic Teston, Proba project manager notes that, "small satellites have proven their worth for rapid testing of spacecraft techniques and onboard instruments. They can also support dedicated missions very efficiently" (SpaceDaily, 2003). A Proba microsatellite is depicted below in Figure 2.

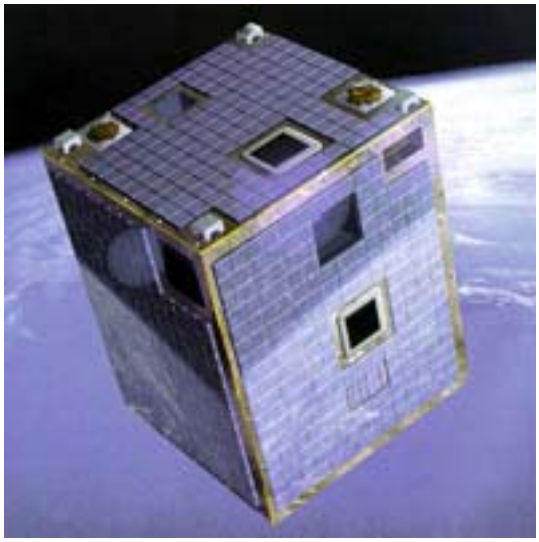

Figure 2. Artist Impression of Proba in Orbit (ESA, 2003)

The Air Force Research Laboratory (AFRL) is currently building and demonstrating microsatellite technologies. Specifically, the Experimental Spacecraft System (XSS) Microsatellite Demonstration Project includes two very applicable missions. These missions are to actively evaluate future applications of microsatellite technologies to include: inspection, rendezvous and docking; repositioning; and techniques for close-in proximity maneuvering around on-orbit assets (XSS-10 Fact Sheet).

XSS-10, launched in January of 2003, commenced an autonomous inspection sequence around the second rocket stage, transmitting live video to ground stations. Key technologies demonstrated include: lightweight propulsion; guidance, navigation and control (GN&C); and integrated camera and star sensor (XSS-10 Fact Sheet). XSS-10

achieved its primary mission by successfully maneuvering from within 100 m to 35 m of the rocket stage, backing away and repeating the process again.

Work on the follow-on vehicle, XSS-11, continues. XSS-11 is to further advance technologies and techniques to increase the level of onboard autonomy. One of the major challenges is in how to sense relative position and velocity when in proximity to another space object (Partch, 2003). The efforts of AFRL confirm the need for complex navigation and orbital guidance algorithms onboard the spacecraft. XSS-11 is illustrated in Figure 3 courtesy of AFRL.

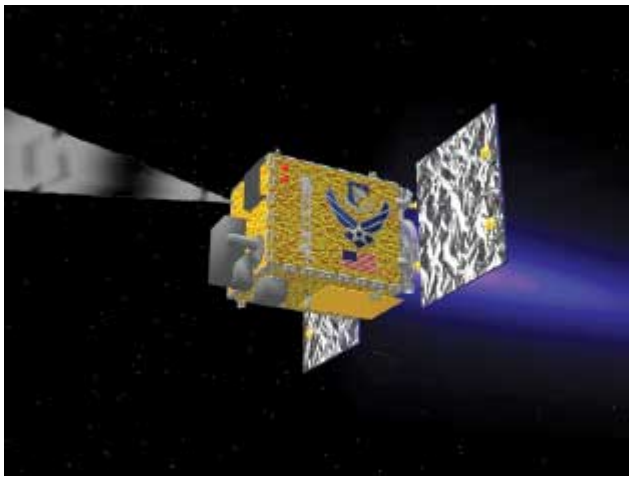

Figure 3. XSS-11 Operating a Low-Power Lidar (Partch, 2003)

XSS-11 is both a fast paced, 30-month, and highly collaborative effort. The Space Vehicles Directorate of AFRL is partnering with Lockheed Martin and Jackson & Tull to build and integrate the microsatellite. It will employ a sophisticated three-axis stabilized platform, advanced propulsion system, and communications subsystems

pushing the scientific envelope. This will all lead to real-time streaming video of the proximity operations being sent to ground operators.

The avionics system is understandably the core of the XSS-11 spacecraft. The radiation hard Power PC 750 processor, develop by AFRL and NASA, enabling the complex data processing, guidance algorithms, and onboard autonomy will encounter its first flight test on XSS-11(Partch, 2003). The challenge of sensing relative position and velocity also required a new material solution. Due to the lack of communication with the target satellite, AFRL had to develop alternative approaches for relative position determination. The active sensing system selected involves a high tech active scanning lidar ranging system. Complementing the active system, XSS-11 will employ a combined visible camera and star tracker passive remote sensing system. Finally, onboard iterative trajectory simulations are coupled with an advanced autonomous event planner, monitor, and forward-thinking resource manger to optimize the timing of rocket firings (Partch, 2003). The development and miniaturization of the above key components required significant joint research, development, and integration.

The above review is only a small sample of current and projected microsatellite activity in industry, academia, and military arenas. It serves to support the argument that microsatellite capabilities will continue to rapidly increase as technical hurdles are overcome. Specific to the non-cooperative rendezvous problem, the work of AFRL is particularly applicable. GN&C technology maturation is an area of intense examination. Advances in miniaturization and the proliferation of space technologies will enable many

less knowledgeable countries to contend, as unsolvable problems of today will be taken for granted tomorrow.

Relevant Research

A wealth of previous research has been conducted at AFIT regarding microsatellite rendezvous and docking operations. Just within the last two years, work related to the selection of tracking and orbit determination architectures; rendezvous control algorithm development; and target satellite dynamics modeling for microsatellite docking detection has been accomplished. A recent American Astronautical Society paper outlining a conceptual design for the GN&C system for a maintenance and repair spacecraft complements the above work.

Control Laws

Troy Tschirhart, a former AFIT master's student, studied the control laws necessary for achieving rendezvous with a non-cooperative target while minimizing fuel requirements. The relative motion of a microsatellite and target satellite were described using Hill's equations and two different controller methodologies were investigated. An impulsive thrust controller based on the Clohessey-Wiltshire solution was found to use little fuel, but was not very robust. A continuous thrust controller using a Linear Quadratic Regulator (LQR) was found to be more robust, but used much more fuel. The algorithm developed for this control method is depicted in Figure 4 below.

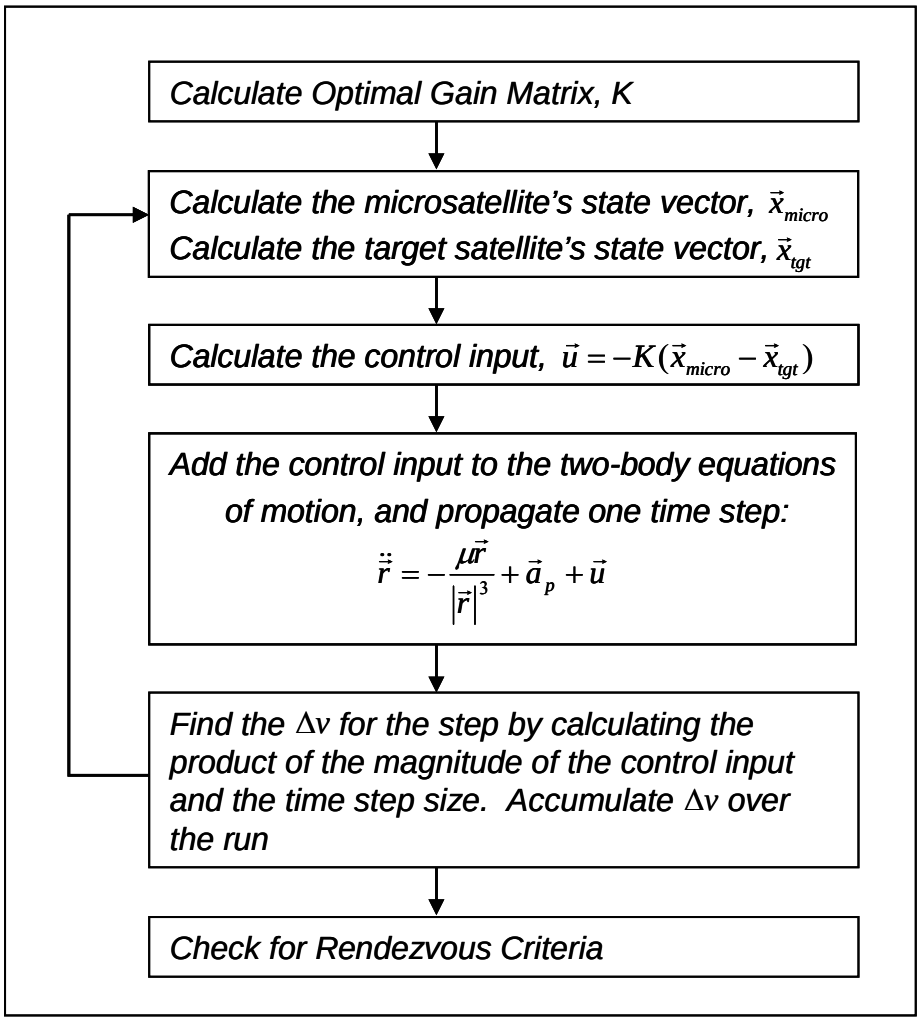

Figure 4. Linear Quadratic Regulator Propagation Algorithm (Tschirhart, 2003)

As a final solution, a hybrid controller was evaluated which uses the low thrust Clohessey-Wiltshire approach to cover most of the necessary distance, and then switches to the Linear Quadratic Regulator method for the final rendezvous solution. Results show that this approach achieves rendezvous with a reasonable amount of control input (Tschirhart, 2003).

This work resulted in a feasible controller algorithm assuming perfect knowledge of the target satellite's state (position and velocity). The Hybrid controller developed achieves rendezvous to the specified relative distance and velocity in 590 minutes, using 48.9 m/s ΔV. The final results of Tschirhart's controller analysis are summarized in Table 1.

Table 1. Tschirhart Controller Results Summary

Controller Type	ΔV (m/s)	Time to Rendezvous (min)
Impusive (CW)	35.75	368*
Continuous (LQR)	383.11	384
Hybrid	48.89	590

*Note: Impulsive Controller does not meet criteria, 3.3 km is closest approach

It is significant to note the Hybrid controller achieved rendezvous with considerable ΔV savings over the LQR controller.

Recommendations for further research included investigating the use of gain scheduling as part of an LQR controller, and the incorporation of a sequential filter. Gain scheduling was suggested in order to lower control usage during the majority of the rendezvous, and then increase it at the end to complete the rendezvous without the complexity of a hybrid controller. A sequential filter was recommended to estimate the state of the target satellite, incorporating realistic uncertainties in using sensor measurements (Tschirhart, 2003).

The LQR controller is of most interest to this researcher given the gain-scheduling recommendation. Therefore the final LQR design results will be reviewed here. Tschirhart used a constant State Weighting Matrix, Q as:

$$Q = \begin{bmatrix} 1 & 0 & 0 & 0 & 0 & 0 \\ 0 & 1 & 0 & 0 & 0 & 0 \\ 0 & 0 & 1 & 0 & 0 & 0 \\ 0 & 0 & 0 & 1 & 0 & 0 \\ 0 & 0 & 0 & 0 & 1 & 0 \\ 0 & 0 & 0 & 0 & 0 & 1 \end{bmatrix} \tag{1}$$

and a constant Control Weighting Matrix, R as:

$$R = \begin{bmatrix} 5e12 & 0 & 0 \\ 0 & 5e12 & 0 \\ 0 & 0 & 5e12 \end{bmatrix} \tag{2}$$

The quadratic cost function:

$$J = \int_0^\infty (x'Qx + u'Ru)dt \tag{3}$$

was then minimized in order to obtain the optimal gain matrix to apply to the control thrust, where x represents the system state (position and velocity) and u is a vector of control inputs.

The controller decreased the relative distance between the microsatellite and target satellite as shown below in Figure 5. The distances in the figure were calculated in the relative reference frame and propagated with the linear equations of motion.

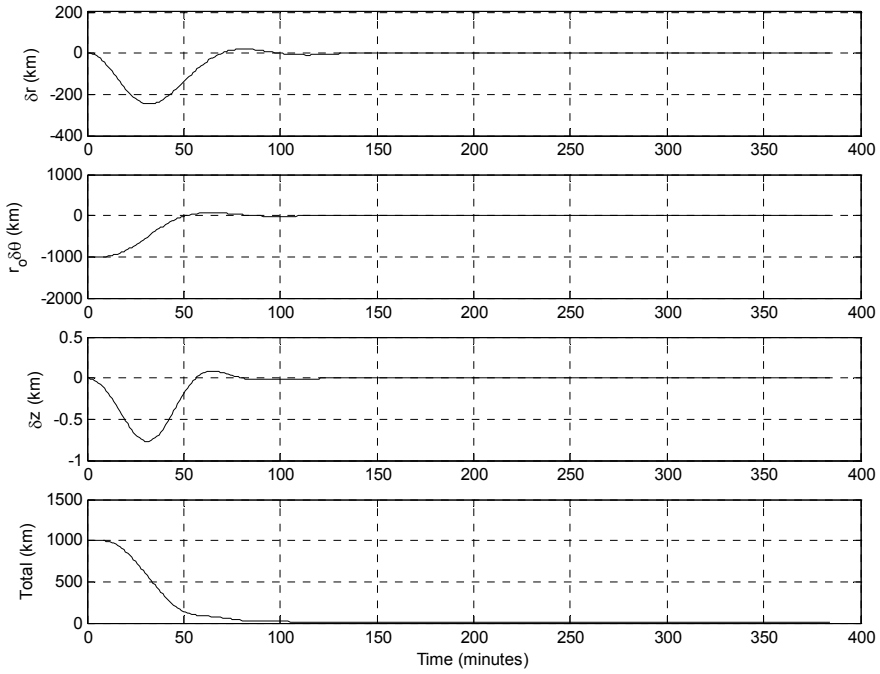

Figure 5. Relative Distance during LQR Rendezvous (after Tschirhart, 2003)

The position of the microsatellite relative to the target, captured in the $\delta r, r_o \delta\theta$ plane is shown in Figure 6. The figure nicely illustrates how the microsatellite initially begins trailing the target by 1000 km in the same orbital plane, and then drops in altitude to increase its speed (i.e. mean motion). Final rendezvous is achieved as the microsatellite arrives within 1 m and 1 cm/s of the target. This particular controller configuration led to the final LQR rendezvous results included in Table 1 above.

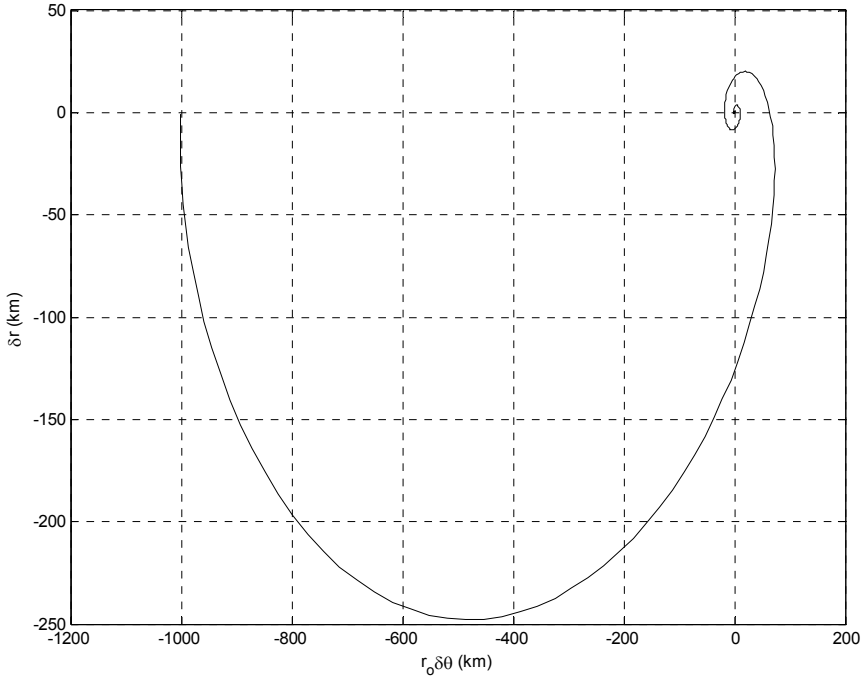

Figure 6. LQR Rendezvous in the $\delta r, r_o \delta\theta$ plane (after Tschirhart, 2003)

Orbit Determination/Navigation

A three-phase tracking system architecture concept and orbit determination routines for non-cooperative rendezvous were developed by another AFIT master's student, Brian Foster. Of particular interest to this research is the on-orbit, third phase, orbit determination routine to estimate the target satellite's orbit. A Non-linear Least Squares orbit determination filter was implemented to accomplish this final phase. As expected, the filter converged to a solution based on simulated data.

The orbit determination filter, as implemented, was found to perform best given a large number of observations which took more collection time and thus would cause

significant processing delays (Foster, 2003). One specific simulation run found the filter was able to reduce the estimate error from an initial 5.2 km to approximately 5 m given 100 data points (sensor observations) separated by 60 seconds each. Less data still allowed the filter to converge on an estimate, but included a much larger error compared to the truth model.

Foster realized that in a rendezvous mission, time to collect and process data may not be available and thus control maneuvers may have to be based on less accurate position estimates. The development of a Kalman-type filter to allow for real-time processing of observation data for the orbit determination process was among the recommendations for future work.

Summary

The study and use of microsatellites to perform a variety of missions is currently underway. It is becoming routine to not only consider small satellites for technology demonstrations, but operational missions as well. Industry is responding to demand by producing creative solutions with applications only bound by human imagination. Previous AFIT research on control laws and orbit determination paved the way for an integrated GN&C analysis.

III. Methodology

Chapter Overview

The purpose of this chapter is two-fold. The first part describes the systems engineering approach taken for this feasibility analysis. This section includes a top-level systems architecture for the potential system being evaluated. The second part details the necessary technical theory required to solve the rendezvous problem. This includes orbital dynamics, control, orbit determination, and estimation theory. The method taken is a top-down systems approach with the majority of effort being spent on the driving GN&C algorithm integration. MathWorks' MATLAB® software was the tool used for the algorithm development and evaluation.

The problem statement specified that the microsatellite will begin approximately 1000 km behind the target in the same orbital plane. In order to better scope this project, the rendezvous has been segmented into phases. The Overarching CONOPS, including the three phases, is in Table 2 below.

Table 2. Overarching CONOPS

Phase	Range Start (km)	Range End (km)	Sensor Used	Purpose
OC-1	1000 km	1000 km	Ground	Obtain Initial Estimate
OC-2	1000 km	5 km	Ground	Initial Rendezvous
OC-3	5 km	1 m	On-Orbit	Final Rendezvous

In Overarching CONOPS Phase 1, OC-1, ground-based sensors would be used to generate an initial target state estimate. Although this early phase would likely require significant global infrastructure to do well, it is not the focus of this research (Foster,

2003). Phase 2 involves closing the relative distance between the microsatellite and target down to 5 km. This value was chosen as it represents the expected outside range of an on-orbit lidar sensor. The control law work of Tschirhart led this researcher to determine this second phase is quite achievable to a reasonable error. The final rendezvous phase, OC-3, is what is studied in detail in this work. The control and estimate accuracy required to achieve rendezvous to within 1 m is certainly the most challenging part of the problem.

Systems Engineering View

There is a distinct difference between traditional, or discipline-specific engineering, and systems engineering. According to Dennis Buede, a well respected expert in the systems engineering field, Engineering is defined as a "discipline for transforming scientific concepts into cost-effective products through the use of analysis and judgment" (Buede, 2000). This often applies best to hardware component or individual software item development. Buede further defines the Engineering of a System to be the "engineering discipline that develops, matches, and trades off requirements, functions, and alternate system resources to achieve a cost-effective, life-cycle-balanced product based upon the needs of the stakeholders" (Buede, 2000). Systems engineering, at a very basic level, is the effort to create an entire integrated system, not just a bunch of components, to satisfy the need.

Taking a systems view involves the up-front planning for and subsequent integration of the traditional engineering products. Many standard tools are becoming available to the systems engineer which result largely in non-material products essential

to system analysis or evaluation. A few concepts applicable to the analysis of a system include an Operational Concept, External Systems Diagram, and a Systems Engineering Architecture.

An Operational Concept often includes a vision for what the system is, a statement of mission requirements, and a description of how the system might be used. Figure 4 below shows three primary choices considered by NASA engineers in determining an Operational Concept for the moon landing during the 1960's (Brooks et al, 1979; Murry and Cox, 1989).

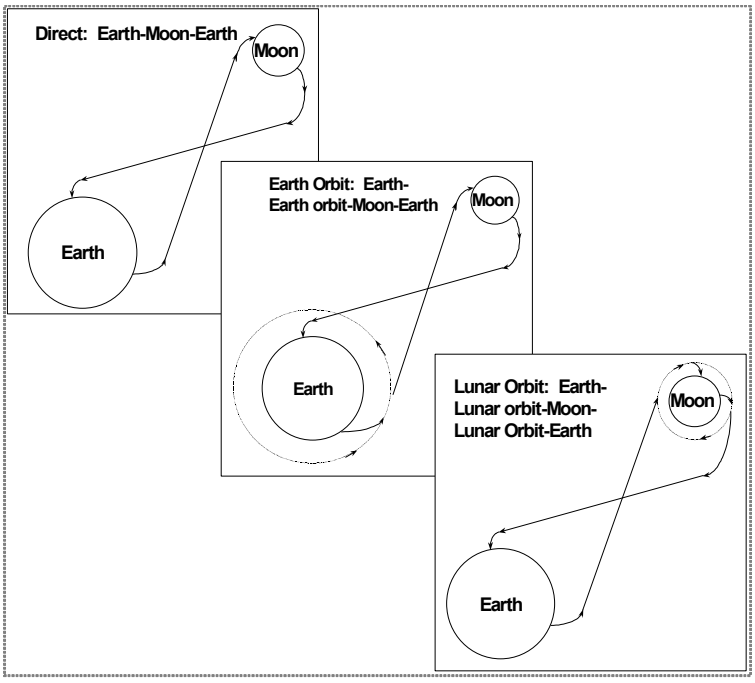

Figure 7. Alternative Concepts for Apollo Moon Landing (Murry and Cox, 1989)

This illustration demonstrates how several potential alternatives may exist for solving a problem. The selection of the most desirable concept(s) is the first step in

evaluating the feasibility of the system. Clearly, if a feasible Operational Concept exists, then it is possible that a material solution can follow. Examples of Operational Concepts that did not work out in practice include those for previous missile defense programs such as the Strategic Defense Initiative, Brilliant Eyes, and Brilliant Pebbles. These cases show that it is not sufficient to have just an Operational Concept. It can identify flaws in initial thinking, but cannot definitively tell you the system will work. More effort is needed for that.

The creation of an External Systems Diagram (ESD) is another useful tool in the design and evaluation of a system. It is a meta-system model of the interaction of the system with other external systems and the relevant context (Buede, 2000). The recognized value of an ESD is in clearly defining system boundaries. Although these boundaries have many useful roles for the systems engineer, for this project they simply help put the system in context to aid in the feasibility assessment. An ESD can be depicted, in its simplest form, as in Figure 8 below. The system itself, external systems, and the context can all be clearly differentiated using a model of this type.

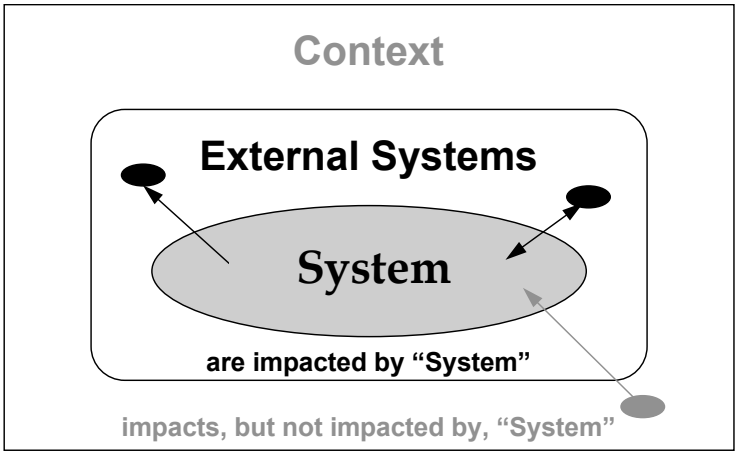

Figure 8. Depiction of the System, External Systems, and Context (Wieringa, 1995)

A Systems Engineering Architecture is useful for creating (i.e. conceptualizing, designing and building) complex, unprecedented systems. Architecting is known to be both an art and a science in both the traditional home building and space system domains. Architectures are not just useful in the development of systems, however. An emerging application is in carrying out behavior and performance analysis and to evaluate potential system designs. Specifically, architectures are beginning to be used to help determine if a proposed system will perform the desired mission in the desired manner, or Operational Concept.

A complete systems architecture is composed of the three views, or perspectives. Figure 9 below illustrates how the Operational, Systems, and Technical Standards Views are combined to fully describe the system.

Figure 9. Architecture Views (DoDAF)

An architecture is developed for a specific purpose and only to the point that useful results are obtained. The right mix of high-level and detail views must be sought for an effective, efficient artifact to result.

The Operational View (OV) includes the tasks, activities, and operational elements. It generally involves both graphic and textual descriptions to convey the concepts and intended uses of the system. The Systems View describes and interrelates the technologies, systems and other resources necessary to support the requirements. The Technical Standards View contains the rules, conventions and standards governing system implementation.

The intent of this research is to develop only the minimum set of architecture products necessary to make a top-level evaluation of system achievability. This researcher has developed three OV products for the system evaluation: High-level Operational Concept Graphic, Operational Concept Narrative, and Functional

Decomposition. Therefore, the Systems and Technical Standards views have not been completed. Although all three views are necessary for a complete systems architecture, the OV is deemed sufficient for this project evaluation.

In formally evaluating a system, the development of the system architecture is just one step in the process. Dr. Alexander Levis, Chief Scientist of the Air Force, outlines an evaluation approach in Figure 10 below. Once an architecture is developed, an executable model must then be constructed and run to develop analysis results. Only a top-level architecture design was developed for this project, therefore only a qualitative evaluation of the system can be made.

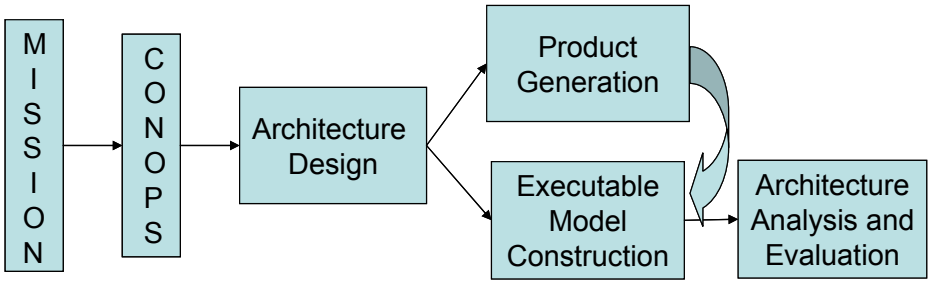

Figure 10. Architecture Evaluation Approach (after Levis, 2003)

Control Theory

This section outlines the orbital dynamics theory applied to the control aspects of the rendezvous problem. Guidance, or orbit control, is defined simply by Wertz as "adjusting the orbit to meet some predetermined conditions" (Wertz, 1999). The conditions in this case are those of a successful rendezvous, nominally within 1 m relative distance and 1 cm/s relative velocity between the microsatellite and target.

Before the details specific to this rendezvous problem are discussed, an interesting historical control system is presented. Perhaps one of the earliest control systems ever employed was by Hero of Alexandria in ancient times. The device for opening his temple doors is shown in Figure 11 below.

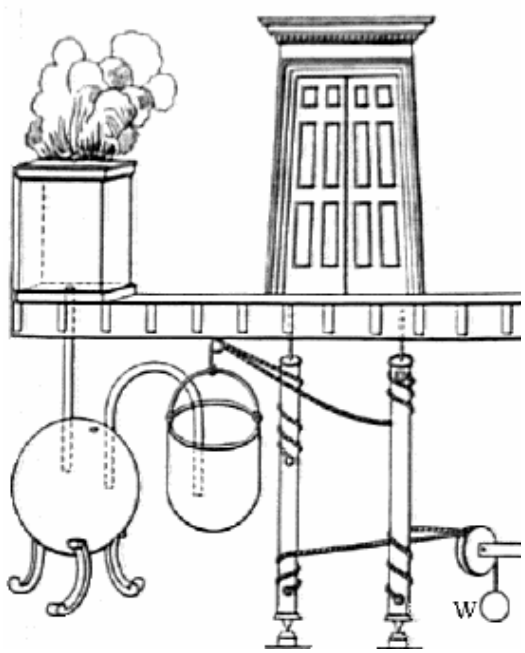

Figure 11. Hero's Control System for Opening Temple Doors

The system input was lighting the alter fire. Water from the container on the left was driven to the bucket on the right by the expanding hot air under the fire. The bucket descended as it became heavier, thus turning the door spindles and opening the doors. Extinguishing the fire had the opposite effect. As the control mechanism was not known to the masses, it created an air of mystery, demonstrating the power of the Olympian gods.

In order to apply the theory to the rendezvous problem, it is necessary to first outline relative motion. This theory describes the microsatellite and target positions and velocities relative to a circular reference frame. Hill's coordinate frame, shown in Figure 12, can aid in illustrating this concept. The origin O is centered in the Earth and fixed in inertial space. O' is the origin of a reference frame that is centered on the instantaneous location of a point moving about O in a circular orbit with mean motion, n. The unit vectors in the circular reference frame (RTZ) are $\hat{e}_r, \hat{e}_\theta, \hat{e}_z$ in the radial, in-track, and out of plane directions, respectively, and r_o is the radius of the circular reference orbit (Tragesser, 2003).

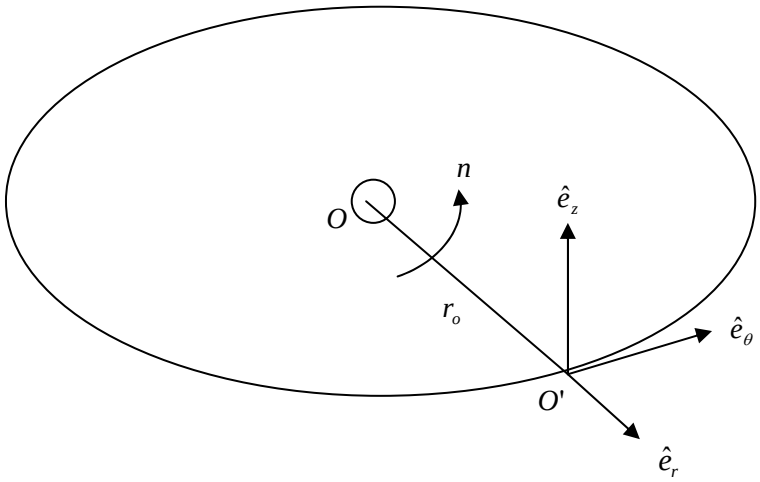

Figure 12. Hill's (RTZ) Coordinate Frame

A satellite can be added to Figure 12, to illustrate the relative position from the reference orbit. Figure 13 below illustrates this relative position in the RTZ coordinate frame.

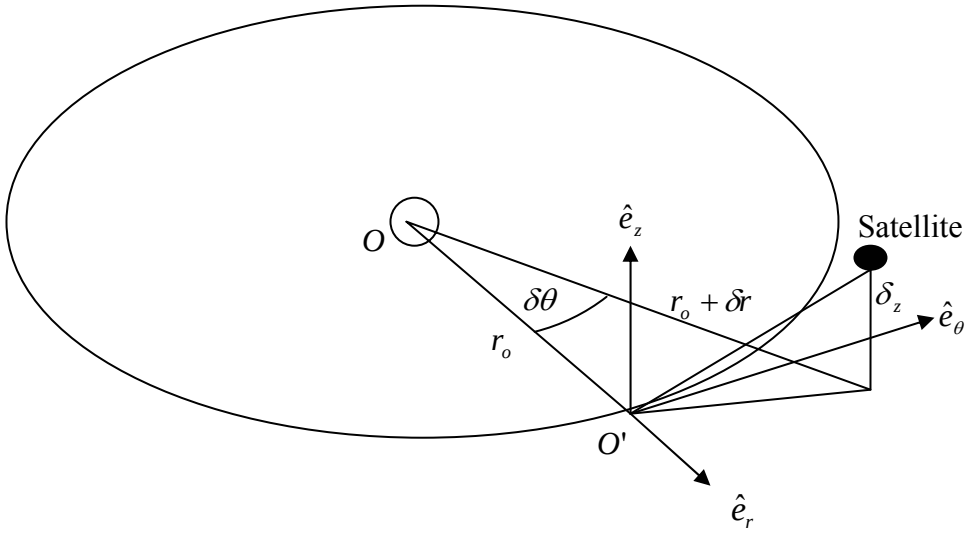

Figure 13. Relative Position in RTZ Coordinate Frame

In this frame, the position of the satellite is:

$$\vec{r} = \left[(r_o + \delta r)\cos\delta\theta\right]\hat{e}_r + \left[(r_o + \delta r)\sin\delta\theta\right]\hat{e}_\theta + \left[\delta z\right]\hat{e}_z \tag{4}$$

and the velocity can be found from:

$$\vec{v} = {}^{i}\frac{d}{dt}(\vec{r}) = {}^{o}\frac{d}{dt}(\vec{r}) + (\vec{n}\times\vec{r}) \tag{5}$$

where the superscripts i and o correspond to the inertial and circular reference frames, respectively, and the mean motion of the circular reference frame is:

$$\vec{n} = \sqrt{\frac{\mu}{r_o^3}}\hat{e}_z \tag{6}$$

Through a fair amount of manipulation, the relative equations of motions follow as in Equation 7.

$$\begin{aligned} \delta\ddot{r} - 2nr_o\delta\dot{\theta} - n^2\left(r_o + \delta r\right) &= -n^2\left(r_o - 2\delta r\right) \\ r_o\delta\ddot{\theta} + 2n\delta\dot{r} - n^2 r_o\delta\theta &= -n^2 r_o\delta\theta \\ \delta\ddot{z} &= -n^2\delta z \end{aligned} \tag{7}$$

Solving Equation 7 yields:

$$\begin{aligned} \begin{bmatrix} \delta r(t) \\ r_o\delta\theta(t) \\ \delta z(t) \end{bmatrix} &= \begin{bmatrix} 3n\sin\psi & 0 & 0 \\ 6n(\cos\psi - 1) & 0 & 0 \\ 0 & 0 & -n\sin\psi \end{bmatrix} \begin{bmatrix} \delta r(0) \\ r_o\delta\theta(0) \\ \delta z(0) \end{bmatrix} \\ &+ \begin{bmatrix} \cos\psi & 2\sin\psi & 0 \\ -2\sin\psi & 4\cos\psi - 3 & 0 \\ 0 & 0 & \cos\psi \end{bmatrix} \begin{bmatrix} \delta\dot{r}(0) \\ r_o\delta\dot{\theta}(0) \\ \delta\dot{z}(0) \end{bmatrix} \end{aligned} \tag{8}$$

and:

$$\begin{aligned} \begin{bmatrix} \delta r(t) \\ r_o\delta\theta(t) \\ \delta z(t) \end{bmatrix} &= \begin{bmatrix} 4 - 3\cos\psi & 0 & 0 \\ 6(\sin\psi - \psi) & 1 & 0 \\ 0 & 0 & \cos\psi \end{bmatrix} \begin{bmatrix} \delta r(0) \\ r_o\delta\theta(0) \\ \delta z(0) \end{bmatrix} \\ &+ \begin{bmatrix} \dfrac{\sin\psi}{n} & \dfrac{2 - 2\cos\psi}{n} & 0 \\ \dfrac{2\cos\psi - 2}{n} & \dfrac{4\sin\psi - 3\psi}{n} & 0 \\ 0 & 0 & \dfrac{\sin\psi}{n} \end{bmatrix} \begin{bmatrix} \delta\dot{r}(0) \\ r_o\delta\dot{\theta}(0) \\ \delta\dot{z}(0) \end{bmatrix} \end{aligned} \tag{9}$$

where $\psi = nt$. In compact form:

$$\left[\delta\bar{v}(t)\right] = \Phi_{vr}\left[\delta\bar{r}(0)\right] + \Phi_{vv}\left[\delta\bar{v}(0)\right] \tag{10}$$

and:

$$\left[\delta\bar{r}(t)\right] = \Phi_{rr}\left[\delta\bar{r}(0)\right] + \Phi_{rv}\left[\delta\bar{v}(0)\right] \tag{11}$$

Equations 10 and 11 describe the relative velocity and position, respectively, of the satellite with reference to a circular reference orbit. For the theory to hold, both the

microsatellite and target must remain sufficiently close to the circular reference orbit (Wiesel, 1997).

The specific controller scheme chosen uses a Linear Quadratic Regulator (LQR) following the successful results of Tschirhart's work. The theory required for implementation follows, based on the relative reference frame in Figure 13 and the relative equations of motion in Equation 7.

A state vector comprising the relative velocity and position can be defined as:

$$\vec{x} = \begin{bmatrix} \delta r \\ r_o \delta\theta \\ \delta z \\ \delta \dot{r} \\ r_o \delta\dot{\theta} \\ \delta \dot{z} \end{bmatrix} \tag{12}$$

and the derivative as:

$$\dot{\vec{x}} = \begin{bmatrix} \delta \dot{r} \\ r_o \delta\dot{\theta} \\ \delta \dot{z} \\ \delta \ddot{r} \\ r_o \delta\ddot{\theta} \\ \delta \ddot{z} \end{bmatrix} \tag{13}$$

The relative equations of motion can be placed in state equation form:

$$\dot{\vec{x}} = A\vec{x} + B\vec{u} \tag{14}$$

where $\vec{u}$ is a vector of control inputs. Equations 7, 12 and 13 can now be used to rewrite Equation 14 as:

$$\begin{bmatrix} \delta\dot{r} \\ r_o\delta\dot{\theta} \\ \delta\dot{z} \\ \delta\ddot{r} \\ r_o\delta\ddot{\theta} \\ \delta\ddot{z} \end{bmatrix} = \begin{bmatrix} 1 & 0 & 0 & 0 & 0 & 0 \\ 0 & 0 & 1 & 0 & 0 & 0 \\ 0 & 0 & 0 & 0 & 1 & 0 \\ 0 & 3n^2 & 2n & 0 & 0 & 0 \\ -2n & 0 & 0 & 0 & 0 & 0 \\ 0 & 0 & 0 & 0 & 0 & -n^2 \end{bmatrix} \begin{bmatrix} \delta r \\ r_o\delta\theta \\ \delta z \\ \delta\dot{r} \\ r_o\delta\dot{\theta} \\ \delta\dot{z} \end{bmatrix} + \begin{bmatrix} 0 & 0 & 0 \\ 0 & 0 & 0 \\ 0 & 0 & 0 \\ 1 & 0 & 0 \\ 0 & 1 & 0 \\ 0 & 0 & 1 \end{bmatrix} \begin{bmatrix} u_r \\ u_\theta \\ u_z \end{bmatrix} \tag{15}$$

A Linear Quadratic Regulator obtains the optimal gain matrix K such that the state-feedback law:

$$\vec{u} = -K\vec{x} \tag{16}$$

minimizes the quadratic cost function:

$$J = \int_0^\infty \left(x'Qx + u'Ru\right)dt \tag{17}$$

The associated Riccati equation is solved for S:

$$SA + A'S - SBR^{-1}B'S + Q = 0 \tag{18}$$

where Q is the State Weighting Matrix and R is the Control Weighting Matrix.

Higher values in the Q matrix speed movement toward the desired state, and higher values in the R matrix reduce control usage (Tschirhart, 2003). The values of Q and R have been selected to follow the forms of Equations 19 and 20 below. The values of q were be set to 1, while r was allowed to vary during the rendezvous process as gain scheduling is implemented.

$$Q = \begin{bmatrix} q & 0 & 0 & 0 & 0 & 0 \\ 0 & q & 0 & 0 & 0 & 0 \\ 0 & 0 & q & 0 & 0 & 0 \\ 0 & 0 & 0 & q & 0 & 0 \\ 0 & 0 & 0 & 0 & q*100 & 0 \\ 0 & 0 & 0 & 0 & 0 & q*100 \end{bmatrix} \tag{19}$$

$$R = \begin{bmatrix} r & 0 & 0 \\ 0 & r & 0 \\ 0 & 0 & r \end{bmatrix} \tag{20}$$

MATLAB's LQR function is used to calculate the optimal gain matrix as:

$$K = R^{-1}B'S \tag{21}$$

The control input of Equation 16 must now be modified to account for the fact the microsatellite is chasing the target rather than the reference. This control should be based on the difference between the microsatellite's state vector and the target's state vector:

$$\begin{bmatrix} u_r \\ u_\theta \\ u_z \end{bmatrix} = -K \begin{bmatrix} \delta r_{micro} - \delta r_{tgt} \\ r_o \delta\theta_{micro} - r_o \delta\theta_{tgt} \\ \delta z_{micro} - \delta z_{tgt} \\ \delta \dot{r}_{micro} - \delta \dot{r}_{tgt} \\ r_o \delta\dot{\theta}_{micro} - r_o \delta\dot{\theta}_{tgt} \\ \delta \dot{z}_{micro} - \delta \dot{z}_{tgt} \end{bmatrix} \tag{22}$$

The LQR routine developed by Tschirhart, outlined in Figure 4, was used to begin this study. The final hybrid controller solution was not examined in favor of implementing gain scheduling in the LQR algorithm. Once better understood, this gain scheduling LQR controller was coupled with different estimation filters, attempting to construct an integrated solution.

Orbit Determination Theory

In using only the above orbital dynamics and control theory to solve the rendezvous problem, perfect knowledge of both the microsatellite and the target must be assumed. One can expect the microsatellite maintains fairly good knowledge of its own state, by using GPS for example. The position and velocity of the target, however, must be estimated in some manner. As in an electrical filter which extracts the desired signal from the undesired, an estimation algorithm which extracts the system state from observations with errors is called a filter (Wiesel, 2003). An observer, or filter, must be designed to estimate the plant states that are not directly observed.

There are various methods of reconstructing the states from the measured outputs of a dynamical system. Estimation filter types relevant to this research include: linear, nonlinear, batch, and sequential. A linear estimator assumes the data is linearly related to the system state at the time taken. This can greatly simplify the problem, but is not applicable in many cases. In a nonlinear estimator, the observed quantities are allowed to be related to the system state by a very nonlinear set of relations (Wiesel, 2003). Another way to classify a filter is via how the data are processed. A batch algorithm assumes all data are available before the estimation process begins, and is all processed in one large batch. A sequential filter is continuously taking in new data and producing an improved estimate. A batch algorithm can be made more sequential by observing and processing smaller batches of data.

An estimate of the target state, $\vec{x}$, will be represented as $\hat{\vec{x}}$. A trajectory to linearize the dynamics about must also be chosen. As the true system state $\vec{x}$ is

unobtainable and an estimate $\hat{\vec{x}}$ does not yet exist, a reference trajectory is used. The reference trajectory, $\vec{x}_{ref}$, is a trajectory one expects will be close to the estimate. The goal is to find corrections to the reference trajectory turning it into a reasonably good estimate, $\hat{\vec{x}}$. The reference trajectory usually comes from an initial orbit determination method and is then updated based on observation data (Wiesel, 2003).

The control law in Equation 16 will be modified as:

$$\vec{u} = -K\hat{\vec{x}} \tag{23}$$

For a linear filter, a reasonable way to estimate $\vec{x}$ is by duplicating the actual state dynamics in propagating $\hat{\vec{x}}$ (Cobb, 2003). The equations of motion for the target as shown in Equation 14 will then be described as:

$$\dot{\hat{\vec{x}}} = A\hat{\vec{x}} + B\vec{u} \tag{24}$$

Since the true target state, $\vec{x}$ cannot be measured, a correction term must be added to the dynamics equation for the observer. Equation 24 can be modified to include a correction term proportional to the difference between the measured and estimated output (Cobb, 2003):

$$\dot{\hat{\vec{x}}} = A\hat{\vec{x}} + B\vec{u} + L(\vec{y} - C\hat{\vec{x}}) \tag{25}$$

where L is the estimator gain matrix, $\vec{y}$ represents the model for the measurement, and C models the observation geometry. The $\vec{y} - C\hat{\vec{x}}$ term represents the filter residuals. This residual term can also be described as the difference between measured and predicted observation values:

$$r_i = z_{measured} - z_{predicted} \tag{26}$$

Shown in the form of Equation 26, it is evident the goal of the filter is to minimize the residual, or correction term.

MATLAB contains a number of built-in linear filters. A simple one to use is LQE. The Linear Quadratic Estimator, or LQE, follows a stationary Kalman estimator design for continuous-time systems. It returns the observer gain matrix L to include in the equation of motion given in Equation 25. A block diagram showing how a Kalman filter can used to form a Kalman estimator is shown in Figure 14.

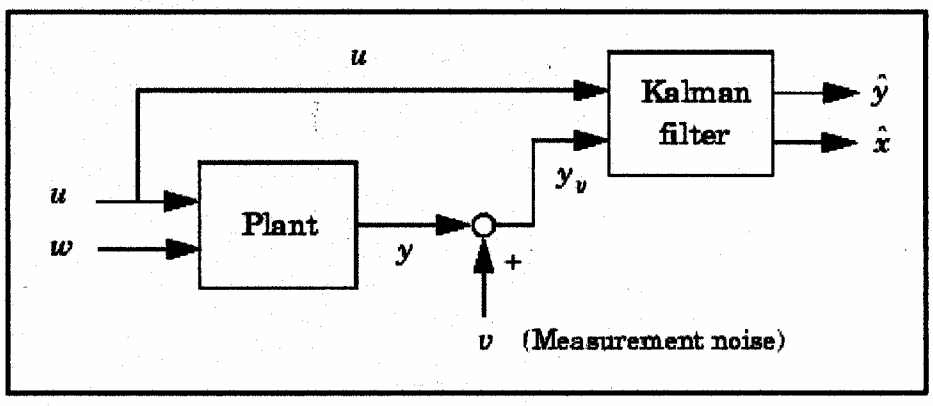

Figure 14. Kalman Estimator (MATLAB)

The MATLAB function LSIM can then be used to simulate the model response, obtaining the state estimate $\hat{x}$. Specifically, the command lsim (sys, u, t) produces a plot of the time response of the LTI model sys to the input time history t, u.

As stated above, a simple linear filter is not sufficient for many control problems. In such cases, a more complex nonlinear estimator may be required. "To handle

problems which are useful in the real world we must abandon the linear case and work with nonlinear system dynamics and the nonlinear observation geometry" (Wiesel, 2003). Wiesel details a very good algorithm for a Non-linear Least Squares estimator in his book *Modern Orbit Determination.* This routine amounts to calculating the state from the observations. The specific steps given by Wiesel are as follows:

1. Propagate the state vector to the observation time t_i and obtain the state transition matrix $\Phi(t_i, t_o)$

   where $\Phi = \begin{bmatrix} \frac{\partial x}{\partial x} & \frac{\partial x}{\partial y} & \frac{\partial x}{\partial z} & \frac{\partial x}{\partial \dot{x}} & \frac{\partial x}{\partial \dot{y}} & \frac{\partial x}{\partial \dot{z}} \\ \frac{\partial y}{\partial x} & \frac{\partial y}{\partial y} & \frac{\partial y}{\partial z} & \frac{\partial y}{\partial \dot{x}} & \frac{\partial y}{\partial \dot{y}} & \frac{\partial y}{\partial \dot{z}} \\ \frac{\partial z}{\partial x} & \frac{\partial z}{\partial y} & \frac{\partial z}{\partial z} & \frac{\partial z}{\partial \dot{x}} & \frac{\partial z}{\partial \dot{y}} & \frac{\partial z}{\partial \dot{z}} \\ \frac{\partial \dot{x}}{\partial x} & \frac{\partial \dot{x}}{\partial y} & \frac{\partial \dot{x}}{\partial z} & \frac{\partial \dot{x}}{\partial \dot{x}} & \frac{\partial \dot{x}}{\partial \dot{y}} & \frac{\partial \dot{x}}{\partial \dot{z}} \\ \frac{\partial \dot{y}}{\partial x} & \frac{\partial \dot{y}}{\partial y} & \frac{\partial \dot{y}}{\partial z} & \frac{\partial \dot{y}}{\partial \dot{x}} & \frac{\partial \dot{y}}{\partial \dot{y}} & \frac{\partial \dot{y}}{\partial \dot{z}} \\ \frac{\partial \dot{z}}{\partial x} & \frac{\partial \dot{z}}{\partial y} & \frac{\partial \dot{z}}{\partial z} & \frac{\partial \dot{z}}{\partial \dot{x}} & \frac{\partial \dot{z}}{\partial \dot{y}} & \frac{\partial \dot{z}}{\partial \dot{z}} \end{bmatrix}$

   and x, y, z refer to the three components of the position vector. The state transition matrix comes from linear dynamical systems, where Φ propagates the actual state as a function of time. It is the gradient of the solution with respect to the initial conditions.

2. Obtain the residual vector $r_i = z_i - G(\vec{x})$, where z_i is the measured observation vector and $G(\vec{x})$ is the predicted data vector of the current state vector $\vec{x}$. Calculate the observation model H_i for this particular data point, where $H_i = \frac{\partial G}{\partial \vec{x}}\Big|_{x_{ref}}$. Then calculate the observation matrix $T_i = H_i \Phi$.

3. Add new terms to the running sums of the matrix $\sum_i T_i^{'} Q_i^{-1} T_i$ and the vector $\sum_i T_i^{'} Q_i^{-1} r_i$

where Q is the total instrument covariance matrix.

When all data has been processed:

4. Calculate the covariance of the correction $P_{\delta x} = (\sum_i T_i^{'} Q_i^{-1} T_i)^{-1}$ and the state correction vector at epoch $\delta x(t_o) = P_{\delta x} \sum_i T_i^{'} Q_i^{-1} r_i$. Note that the matrix $T_i^{'} Q_i^{-1} T_i$ must be invertible for a new estimate of the reference trajectory to exist. This is known as the observability condition.

5. Correct the reference trajectory $x_{ref+1}(t_o) = x_{ref}(t_o) + \delta x(t_o)$. x_{ref+1} is the new estimate of the reference trajectory.

6. Determine if the process has converged. If not, begin again at step 1. If so, x_{ref} is an estimate with covariance P_x.

7. Check to ensure there are no unbelievably large, greater than 3σ , residuals. If so, reject the observation in step 3.

Typical observation measurements are of the form: range; range and range rate; range, azimuth and elevation. The measurements chosen for this research include range, azimuth and elevation. The observations z_i can then be described as:

$$\vec{z}_i = \begin{bmatrix} range \\ azimuth \\ elevation \end{bmatrix} = \begin{bmatrix} \rho \\ \alpha \\ \beta \end{bmatrix} = \begin{bmatrix} \sqrt{x^2 + y^2 + z^2} \\ \tan^{-1}\left(y/x\right) \\ \tan^{-1}\left(z/\sqrt{x^2 + y^2}\right) \end{bmatrix} \tag{27}$$

As the predicted observation value $G(\vec{x})$ takes the same form as $\vec{z}_i$, the observation model $H_i = \left.\frac{\partial G}{\partial \vec{x}}\right|_{x_{ref}}$ components are given by:

$$H_{11} = \frac{x}{\rho} \tag{28}$$

$$H_{12} = \frac{y}{\rho} \tag{29}$$

$$H_{13} = \frac{z}{\rho} \tag{30}$$

$$H_{21} = \frac{\frac{-y}{x^2}}{1+\left(\frac{y}{x}\right)^2} \tag{31}$$

$$H_{22} = \frac{\frac{1}{x}}{1+\left(\frac{y}{x}\right)^2} \tag{32}$$

$$H_{23} = 0 \tag{33}$$

$$H_{31} = \frac{\frac{-xz}{\left(x^2+y^2\right)^{3/2}}}{\left(1+\frac{z^2}{\left(x^2+y^2\right)}\right)} \tag{34}$$

$$H_{32} = \frac{\frac{-yz}{\left(x^2+y^2\right)^{3/2}}}{\left(1+\frac{z^2}{\left(x^2+y^2\right)}\right)} \tag{35}$$

$$H_{33} = \frac{\frac{1}{\left(x^2+y^2\right)^{1/2}}}{\left(1+\frac{z^2}{\left(x^2+y^2\right)}\right)} \tag{36}$$

and all other components equal to zero. H_i is found by taking the partial derivatives of the G vector with respect to the state, evaluated on the reference trajectory.

In non-linear filter design, one also needs to decide how sequential to make it. The work of Foster was based on a strictly batch method, assuming all data are available

and processed at once. This is generally fine for many applications. For the rendezvous problem at hand, however, it would likely take too long to accumulate all the desired observation data and process before making an update to the target estimate. Waiting for this batch process, the uncertainty in the estimate continues to grow as the target and microsatellite orbit the earth. Care must be taken, however, to not design a "fly-follower" which may attempt to produce a new estimate given only a few observations.

The above discussion relates to watching the covariance of the estimate, which grows during propagation. It also tends to get smaller given new data. This effect is shown in Figure 15, where the state covariance grows between updates and drops when updated.

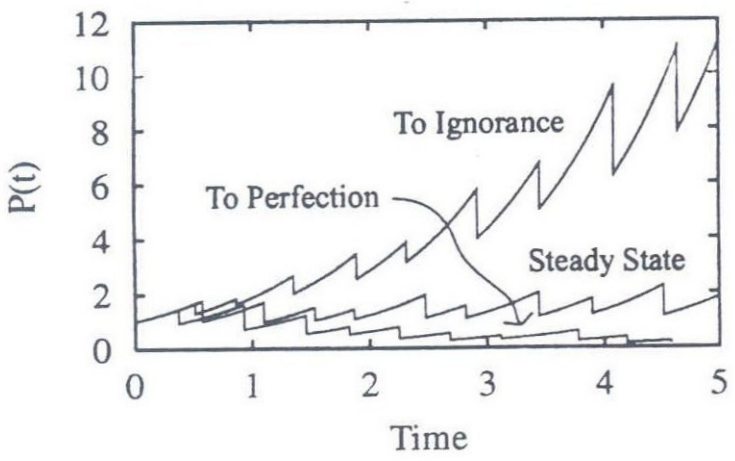

Figure 15. Covariance Behavior with Time (Wiesel, 2003)

If the filter behavior is as the top line "To Ignorance," it fails as the knowledge of the current system state becomes more and more uncertain. If behaving as "To Perfection,"

the filter believes it has achieved perfection and will cease to update the estimate even given new observation data. This condition is often referred to as smugness as the filter will not react to additional input. Neither of the above two conditions is desirable and avoiding them is an art of filter design.

Summary

This chapter outlined the Systems Engineering approach taken to evaluate the non-cooperative rendezvous. An Operational Concept, External Systems Diagram, and Architecture were described as tools to assess top-level system feasibility. A Linear Quadratic Regulator was discussed in context of orbit control laws. Both linear and non-linear filter theory was given to estimate the target state. Wiesel's Non-Linear Least Squares algorithm was detailed as a specific filter routine. Finally, a few subtle filter design considerations were discussed.

IV. Analysis and Results

Chapter Overview

This chapter contains the developed systems engineering products, technical GN&C algorithm analysis, and subsystem integration results. The systems architecture and associated products developed are a necessary, but insufficient, step in the feasibility evaluation. Assessment of the select products indicates top-level system feasibility while underscoring technical and integration complexity.

Beginning the technical study, previous control law development was extended, by gain-scheduling, to show positive trade space between time-to-rendezvous and fuel usage. Given this positive result, attention was focused on the orbit determination filter. The use of a linear estimator is shown to be inappropriate, while a nonlinear estimator requires advanced implementation for the application. Integration of tailored controller and estimator components proved to be beyond the limits of text book algorithms. It would be a non-trivial task to improve these algorithms to account for the necessary complex orbital dynamics involved.

Extending this result leads to a low probability of designing, building, and operating a microsatellite to rendezvous with non-cooperative targets, using established GN&C software routines, in the very near term. A systems or technical view is insufficient to show feasibility by itself. The details that follow show how one view leads to possible attainment, while the other points to serious challenges.

Systems Engineering Front-end Results

Operational Concept

There are a number of ways in which a satellite can perform a non-cooperative rendezvous with a target satellite. The chase satellite can be directly launched to rendezvous or it can perform orbit transfers from a similar orbit as the target. In the latter case, trades are available between on-orbit and ground sensor/processing activities. Three alternative Operational Concepts are depicted in Figures 16-18 below.

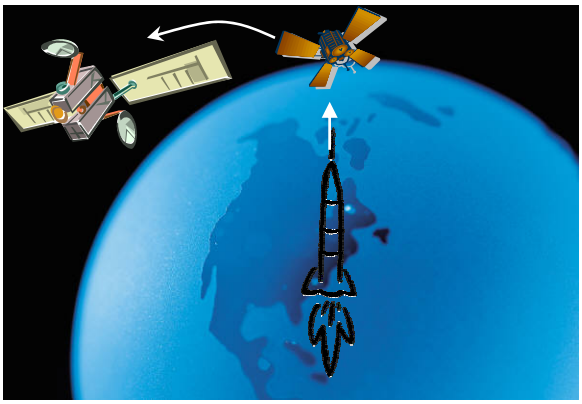

Figure 16. Launch to Rendezvous Ops Concept

The launch to rendezvous concept depicted in Figure 16 above, involves critically determining the launch timing of the chase satellite. The most efficient way to rendezvous in this manner is to launch when the target orbit passes directly over the launch site. Any deviations from the perfect launch time can result in very costly orbit-plane changes. The costs are not only in required weight for propulsion fuel, but also in design complexity. This concept is relatively complicated and difficult to execute. In

order to accomplish the rendezvous directly, without any on-orbit maneuvers, extreme launch precision is required. This further requires very precise knowledge of the target state. Given the above prerequisites, the direct launch to rendezvous operational concept may not represent a low tech solution very well.

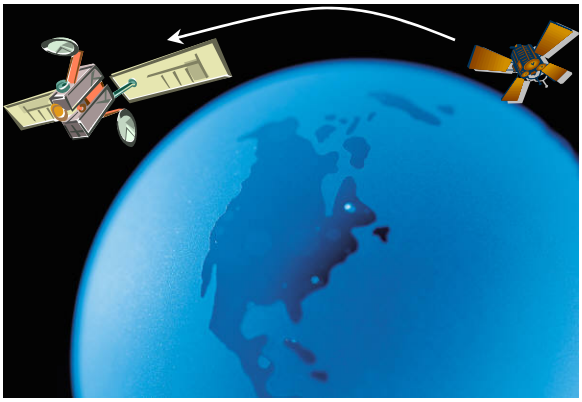

Figure 17. Autonomous Rendezvous Ops Concept

For the autonomous rendezvous, Figure 17, the chase satellite would perform the necessary orbit determination and control activities once given an initial target state estimate from the ground segment. Radar and/or optical ground satellite tracking stations would be required to perform initial orbit determination, but then yield to on-orbit sensors once available. Nominally, only the final 5 km of rendezvous would be performed completely autonomously by the chase satellite. This is primarily limited by sensor performance characteristics. The autonomous rendezvous concept still requires launch to a similar orbit as the target, just not requiring the exactness of the direct launch concept.

As long as the chase vehicle is placed into the same orbital plane, trailing the target by some reasonable amount, the autonomous rendezvous concept retains great potential.

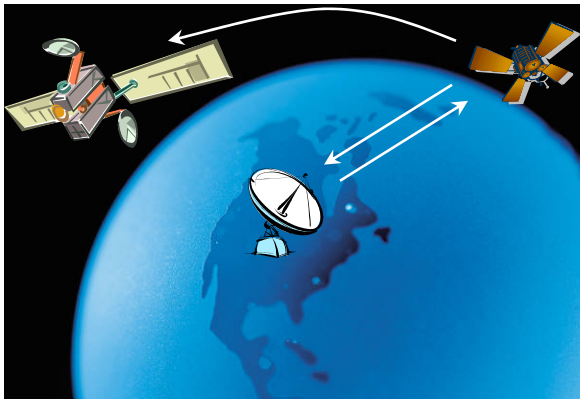

Figure 18. Ground-Assist Rendezvous Ops Concept

A concept using ground sensors and algorithms for the entire rendezvous is shown in Figure 18. Whereas the previous concept only used ground resources for the initial orbit determination, this scheme relies on ground input for the entire rendezvous sequence. This involves extensive development and infrastructure on the ground, but relatively little on the chase satellite. The satellite would receive specific GN&C and propulsion commands to execute each rendezvous maneuver. This alternative may alleviate some of the spacecraft development challenges. The comprehensive ground infrastructure required, however, may also be beyond a low tech approach.

Recalling from the problem statement, the microsatellite is set to begin in the same orbital plane, approximately 1000 km behind the target satellite. The microsatellite then performs rendezvous maneuvers to approach the target. Therefore the autonomous

and ground-assist approaches seem to be more appropriate than the launch to rendezvous concept. The latter could be revisited, however, if other alternatives failed to produce an acceptable solution. The above work establishes that there is adequate trade space to more fully define a final Operational Concept and thus a material solution may exist.

External Systems Diagram

The first step taken in developing an External Systems Diagram was to determine the first-order functions of the system. Defining the top-level function of the system to be "Rendezvous with Target," three additional sub-functions were determined. The high-level functional decomposition, in Figure 19 below, shows acquiring the target state, and determining and executing ΔV maneuvers as sub-functions. This simple decomposition contains functions allocated principally to propulsion and GN&C subsystems.

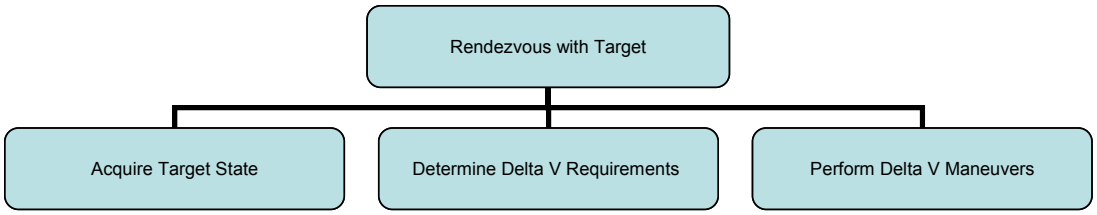

Figure 19. High-Level Functional Decomposition

The standard process modeling technique, IDEF0 (Integrated Definition for Function Modeling), was used to develop the External Systems Diagram (ESD). The decomposition above was used as a starting point to begin the process. Each of the three

sub-functions was identified as an activity in the ESD. Input, outputs and controls (triggers) were then established for each activity function. The resulting diagram in Figure 20 definitively displays the transformation of inputs into outputs by the system.

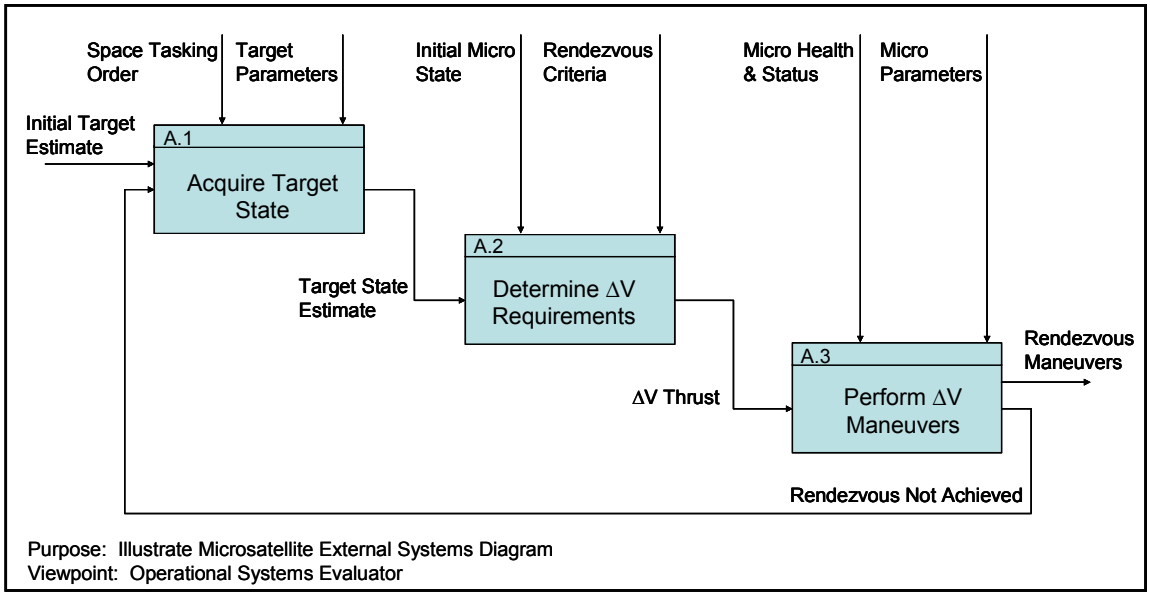

Figure 20. Rendezvous External Systems Diagram

The system boundary is not yet explicitly clear from Figure 20, however. Therefore, a second system ESD was developed following the construct of Figure 8. The system as represented in Figure 21 is better differentiated from the environment, both external systems and context. In this diagram, ground-based sensors and computing resources, support systems and the target satellite are depicted as external systems which interact with the microsatellite. The context, space environment, acts on the microsatellite system, but is clearly not impacted by the system.

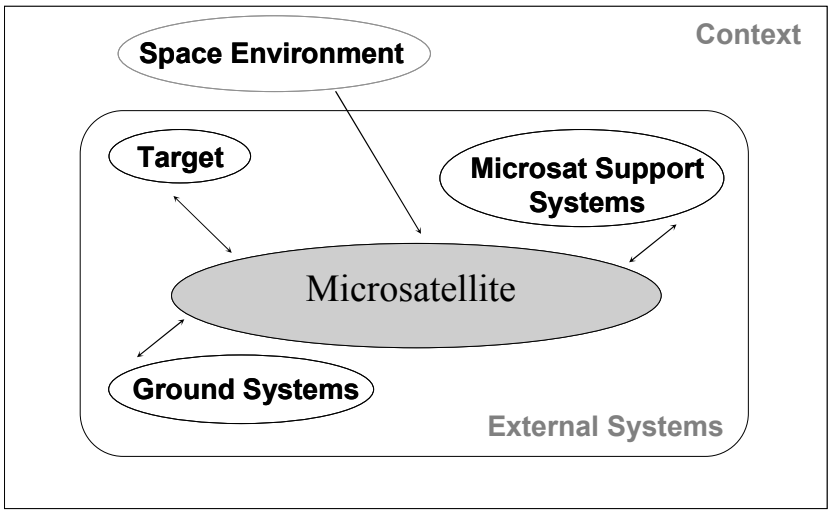

Figure 21. System External Systems Diagram

Even though both External System Diagrams developed are relatively simple, they do help scope the system and are a necessary prerequisite to system architecture creation.

Systems Engineering Architecture

A few top-level systems architecture products have been developed to illustrate one possible microsatellite architecture to achieve a non-cooperative rendezvous. The products include an Operational Concept Graphic, accompanying Narrative, and a detailed Functional Decomposition. Taken together, they document a rough Operational View of the architecture. As stated in the methodology, only a qualitative assessment can be made based on these products. The necessary executable models to base a quantitative assessment on are well beyond the scope of this research.

Operational Concept Graphic

The High-Level Operational Concept graphic for the microsatellite system is shown in Figure 22. The Operational Concept Narrative that follows describes in more detail the interactions between the entities portrayed in the graphic.

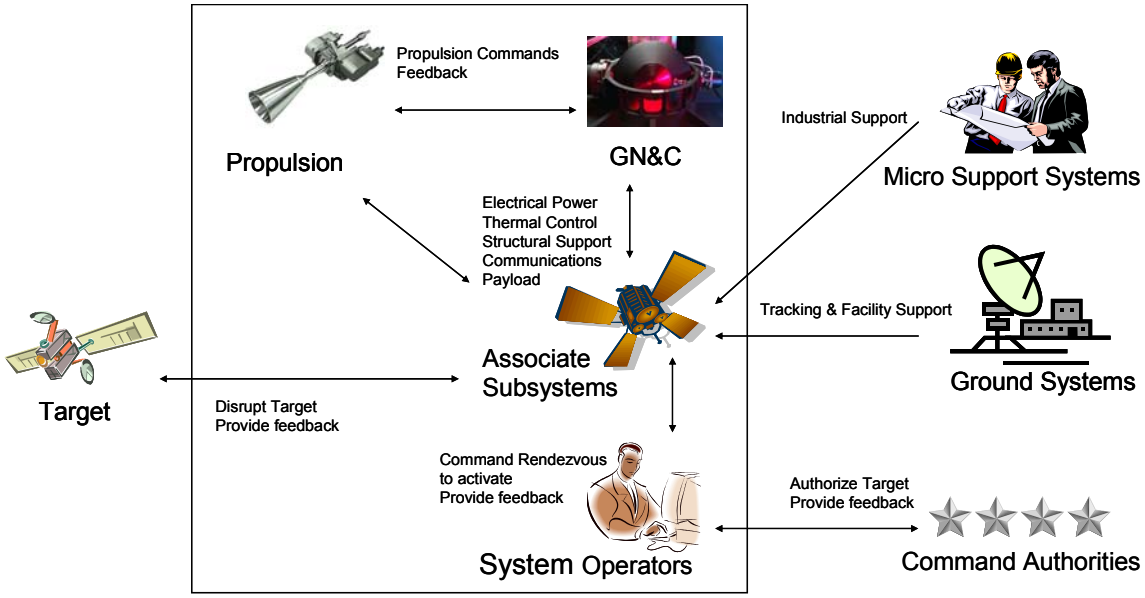

Figure 22. High-Level Operational Concept Graphic

Operational Concept Narrative

The researcher considered a key thread to describe the Operational Concept – the sequence of activities that take place when a user authorizes the Microsatellite System to rendezvous for the purpose of disabling the Target satellite. The architecture is, at this point, proceeding forward assuming the Autonomous Rendezvous Ops Concept alternative depicted in Figure 17.

In order to further bound the system, the key external systems and internal system components need to be identified. The internal system components of the Microsatellite System include the items within the boxed part of the graphic. They include the GN&C, Propulsion, Associated Subsystems, and System Operators. GN&C and Propulsion subsystems are called out separately from other "Associated Subsystems" due to their strong relationship to the activities in the Rendezvous ESD of Figure 20.

System Operators are also drawn inside the box due to dependency on them for non-autonomous operations. It is tempting to exclude the personnel from the system and only evaluate the hardware. The researcher has elected to create the OV architecture products including operators to provide a better system evaluation.

Key external systems include the Target, Command Authorities, Ground and Support Systems. The graphic depicts how these systems interface with the Microsatellite System to include nominal activities.

The rendezvous process can be described as follows: Command Authorities determine a Target requires disabling. This requirement is sent to the Microsatellite System Operators via a Space Tasking Order (STO). The System Operators send a target acquire command to the Microsatellite Associate Subsystems. The Microsatellite then acquires the Target state estimate, initially via Ground Systems. The Microsatellite then begins the rendezvous maneuver, or ΔV calculations. Once determined, the thrust requirements are sent to the Propulsion system to execute. The target state acquisition through propulsion thrust loop continues based on Ground System tracking until the Microsatellite is within range of its on-board tracking sensor.

Once within range, nominally 5 km, the Microsatellite switches to autonomous mode for closed-loop tracking and control. The target acquisition/propulsion thrust sequence continues as before, but now based on space-based sensor measurements, until rendezvous is achieved. When rendezvous is achieved, Associate Subsystems are engaged to disable the identified target. The disabling activity is outside the scope of this architecture and thus will not be detailed. Finally, System Operators generate a mission report for Command Authorities.

Functional Decomposition

Given the External Systems Diagrams and Operational Concept presented above, it is now possible to further detail the initial, high-level, functional decomposition shown in Figure 19. Whereas, the high-level decomposition facilitated ESD development, a more detailed decomposition is required to better evaluate the potential architecture. The detailed functional decomposition is shown in Figure 23.

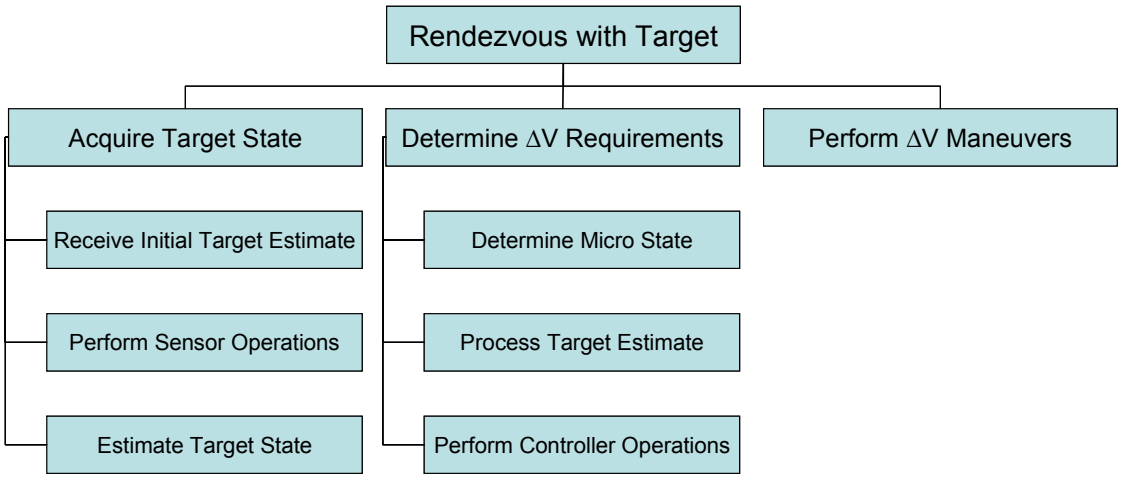

Figure 23. Detailed Functional Decomposition

Only two of the three initial sub-functions, Acquire Target State and Determine ΔV Requirements were further decomposed. The third sub-function, Perform ΔV Maneuvers, did not require such due to the relative simplicity of this function compared to the other two. Each of the lowest-tier function could again be decomposed, but is not necessary for the purpose of this architecture evaluation.

Analyzing the functional decomposition of Figure 23, two conclusions can be drawn. First, the top-level function, Rendezvous with Target, quite easily decomposes into logical sub-functions of necessary depth and breadth to create a more detailed architecture. This lends support to system feasibility at a very broad level. Second, by analyzing the lowest-level sub-functions, it becomes apparent that a collection of complex, integrated activities must take place to perform the rendezvous mission. The two functions decomposed to the lowest level, Acquire Target State and Determine ΔV

Requirements, are physically allocated to the GN&C subsystem. The following sections provide the results of detailed GN&C algorithm analysis.

Controller Gain-Scheduling Results

The first technical area investigated was improving the controller developed by Tschirhart. Although the impulsive/continuous burn hybrid model achieved a relatively efficient rendezvous, implementing a gain-scheduling LQR-only controller offered potential improvement with less complexity. Thus, the State and Control Weighting matrices of Equations 19 and 20, respectively, were examined.

To achieve more efficient control, one desires less control (larger R or smaller Q) initially, and more control (larger Q or smaller R) as the relative distance is reduced. This allows larger ΔV maneuvers to achieve final rendezvous, while avoiding such costly maneuvers early in the process. Only one weighting matrix needs to change to attain the desired result. The Q matrix was left constant while the R matrix was programmed to decrease over time. The Control Weighting Matrix was set to vary as:

$$R = \begin{bmatrix} r_{mag} & 0 & 0 \\ 0 & r_{mag} & 0 \\ 0 & 0 & r_{mag} \end{bmatrix} \tag{37}$$

where

$$r_{mag} = (r_{fin}) * (dist\_now)\text{^}(R\_factor), \text{ for } dist\_now > 1\text{km} \tag{38}$$

$$r_{mag} = r_{fin}, \text{ otherwise} \tag{39}$$

and $dist\_now$ is the relative distance between the two satellites. This part of the study involved varying both the final magnitude of r (r_{fin}), and R_factor.

Reasonable trade space was discovered between the ΔV required and the Time to Rendezvous. The results are summarized below in Table 3.

Table 3. Gain-Scheduling Controller Results

Case	R_fin	R_factor	ΔV (m/s)	Time to Rendezvous (min)
Baseline	5.00E+12	N/A	383.11	384
0-A	5.00E+12	1.00	73.63	524
1-A	1.00E+11	1.00	177.32	245
1-B	1.00E+11	2.00	34.99	572
1-C	1.00E+11	2.50	15.89	1128
2-A	1.00E+12	1.00	112.80	384
2-B	1.00E+12	2.00	19.68	933
2-C	1.00E+12	2.50	9.39	1929
3-A	2.00E+12	1.00	93.73	415
3-B	2.00E+12	2.00	16.66	1089
3-C	2.00E+12	2.50	8.06	2170

The Time to Rendezvous and the ΔV required have, in general, an inverse relationship. This is due to the rendezvous time primarily being driven by the Control Weighting Matrix, R. As a larger R causes rendezvous to be achieved quicker, more fuel is consumed. This correlation is illustrated in Figure 24.

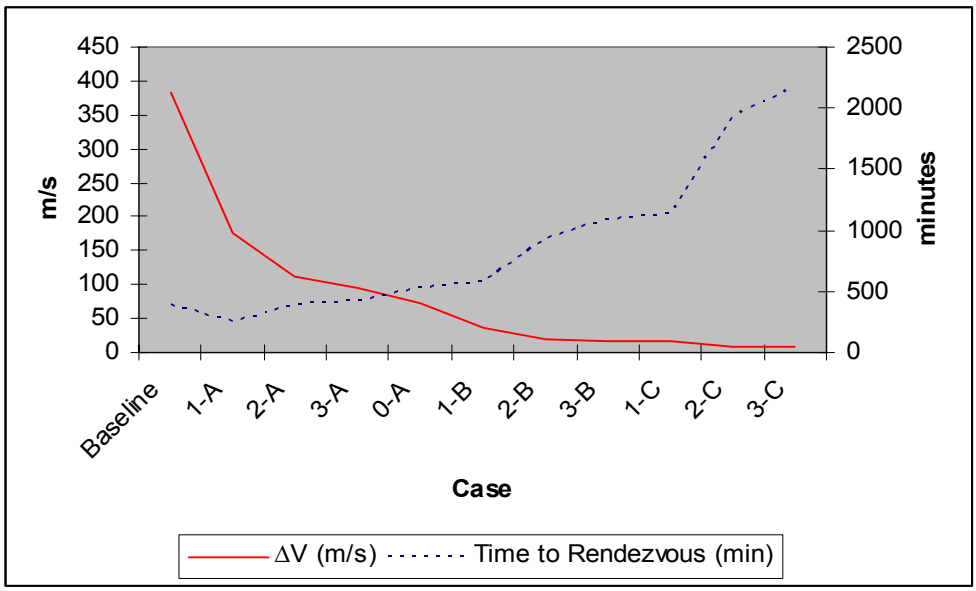

Figure 24. Gain-Scheduling Trade Results

The Gain-Scheduling trade resulted in a controller that can be both more fuel efficient and obtains rendezvous quicker than the hybrid controller developed by Tschirhart, while maintaining flexibility. Case 1-B, for example, achieved rendezvous in 572 minutes, using 34.99 m/s ΔV. This case exhibited fuel performance slightly better than the Impulsive thrust and Hybrid Controller, and an order of magnitude better than the Continuous Non-Gain-Scheduled LQR model shown in Table 1. The Time to Rendezvous was slightly better than the Hybrid Controller, while taking a few additional earth orbits over the Non-Gain-Scheduled LQR Controller. The related performance results are given below in Figures 25 and 26.

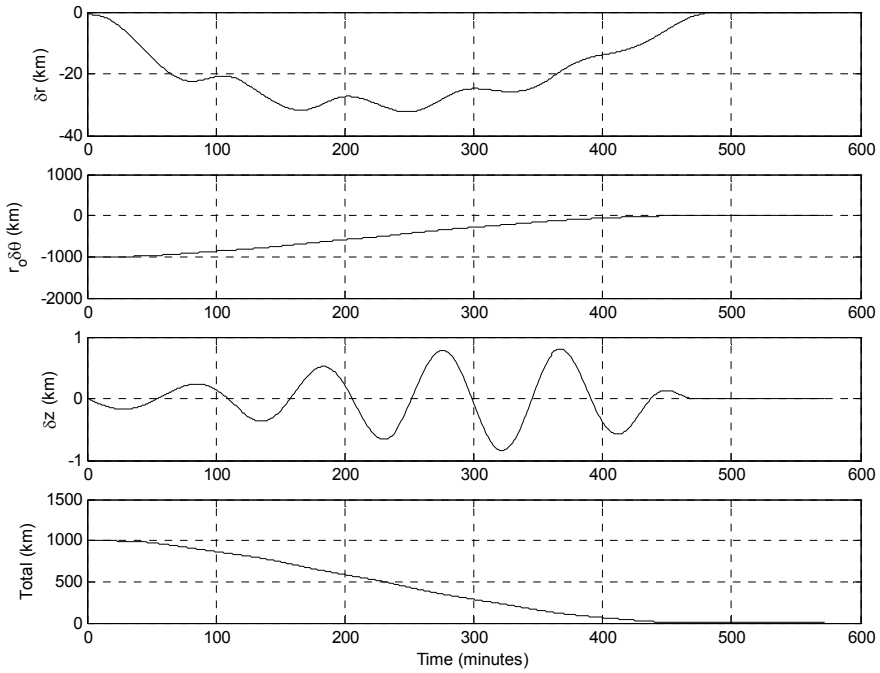

Figure 25. Relative Distance during LQR Rendezvous – Case 1-B

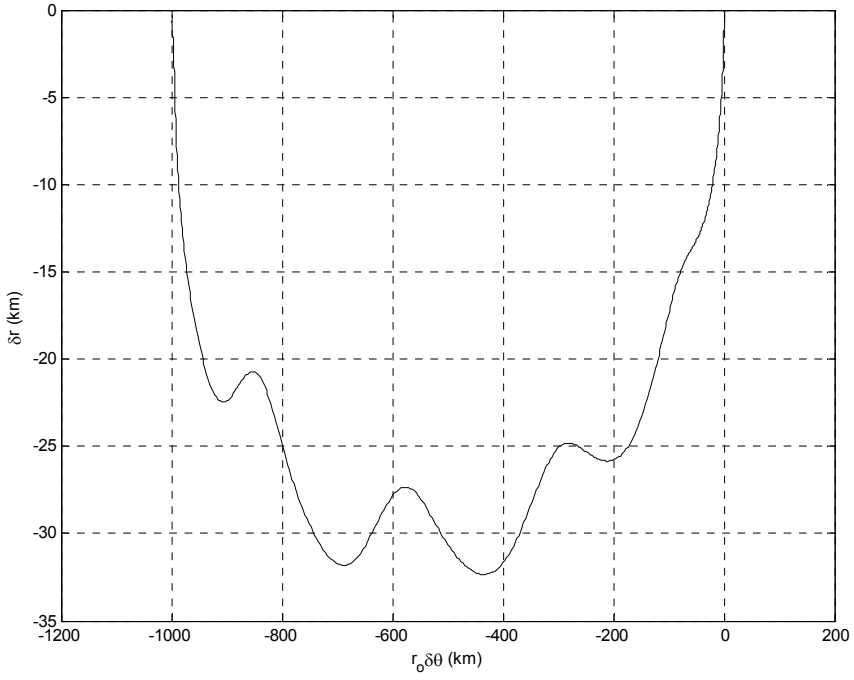

Figure 26. LQR Rendezvous in the $\delta r, r_o \delta\theta$ plane – Case 1-B

Although the results in Table 3 are only a subset, they show adequate trade space exists between the Time to Rendezvous and ΔV requirements. The Baseline Case represents the Non-Gain-Scheduled LQR solution developed by Tschirhart. The subsequent cases all used some level of gain scheduling, as listed in Table 3, to alter the dependent variables. Higher values of r_{fin} and R_factor than are listed were found to either not converge or at least take too long, making them essentially not constructive. The main MATLAB routine is included in Appendix A.

Controller/Estimator Integration

Linear Filter

A simple linear estimator was attempted to integrate with the Gain-Scheduling Controller developed above. In order to first acquire an appreciation for the MATLAB LQE and LSIM tools, a very straightforward estimator was developed. The code is in Appendix B. For this model, the equations of motion in Equation 15, with the control vector set to zero, and an Observation Geometry Matrix, C containing range, azimuth, and elevation were used to obtain the estimator gain matrix, L by LQE command. LSIM was then used to calculate the target and target estimate states over time. This is an open-loop simulation, of the target only, to characterize the performance of a simple linear estimator.

The first simulation began with the target state estimate and target state equal. That is, target knowledge error was set to zero. The initial target state vector, in the form of Equation 12 was given by:

$$\vec{x} = \begin{bmatrix} \delta r \\ r_o \delta\theta \\ \delta z \\ \delta \dot{r} \\ r_o \delta\dot{\theta} \\ \delta \dot{z} \end{bmatrix} = \begin{bmatrix} 1 \\ 0 \\ 0 \\ 0 \\ 0 \\ 0 \end{bmatrix} \tag{40}$$

The simulation was run for 10,000 seconds. The resulting target position and velocity errors are plotted in Figures 27 and 28. Note the state estimates appear to track the truth in all cases throughout the simulation. Data taken at the end of the simulation show the total target position error, 6.16e-004 m, and the total velocity error, 1.76e-006 m, confirm

the visual conclusion. These values are reasonably small as expected, given the perfect initial guess for the state. In fact, the values are indistinguishable in the figures below.

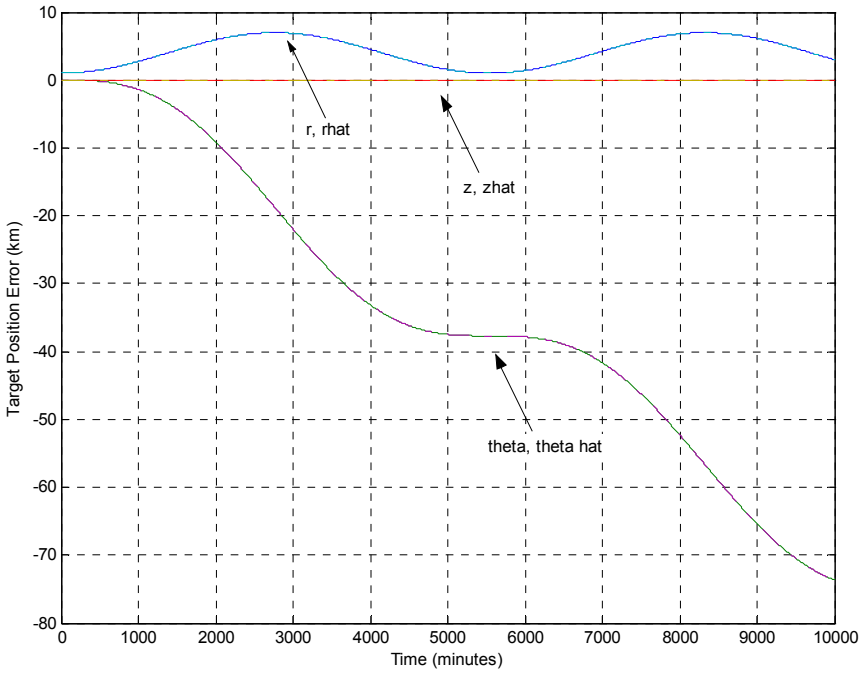

Figure 27. LQE/LSIM Target Position Error with Perfect Initial Estimate

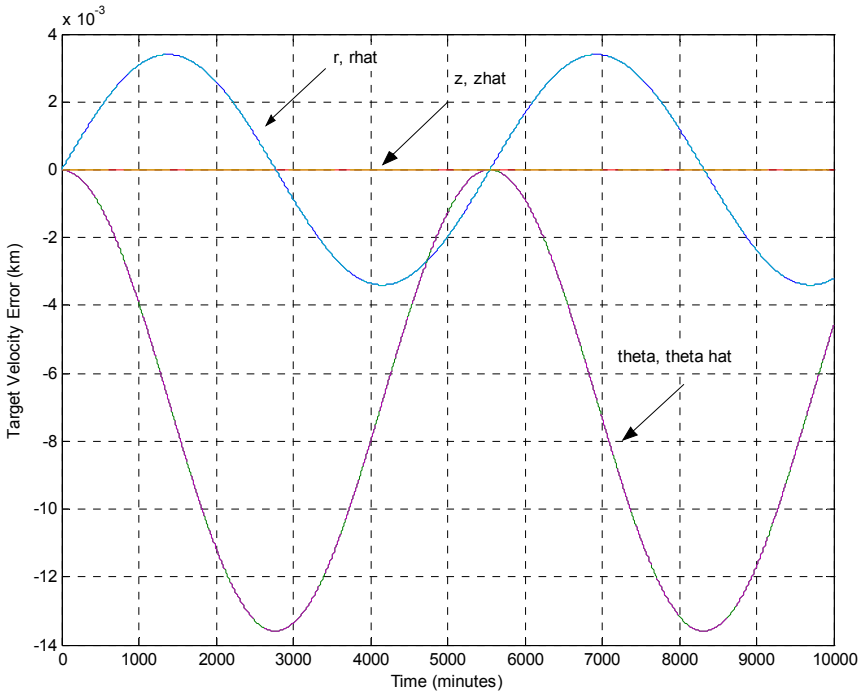

Figure 28. LQE/LSIM Target Velocity Error with Perfect Initial Estimate

Given the estimator will not likely begin with a perfect initial guess, a 1 km target position error was introduced. The 1 km value was assessed as the best an initial orbit determination method could produce as a starting point for any on-orbit estimation (Foster, 2003). Using the same procedure as above, the target knowledge error was set to 1 km, split evenly between the $\hat{e}_r$ and $\hat{e}_\theta$ components. The filter performance for this case is given in Figures 29 and 30.

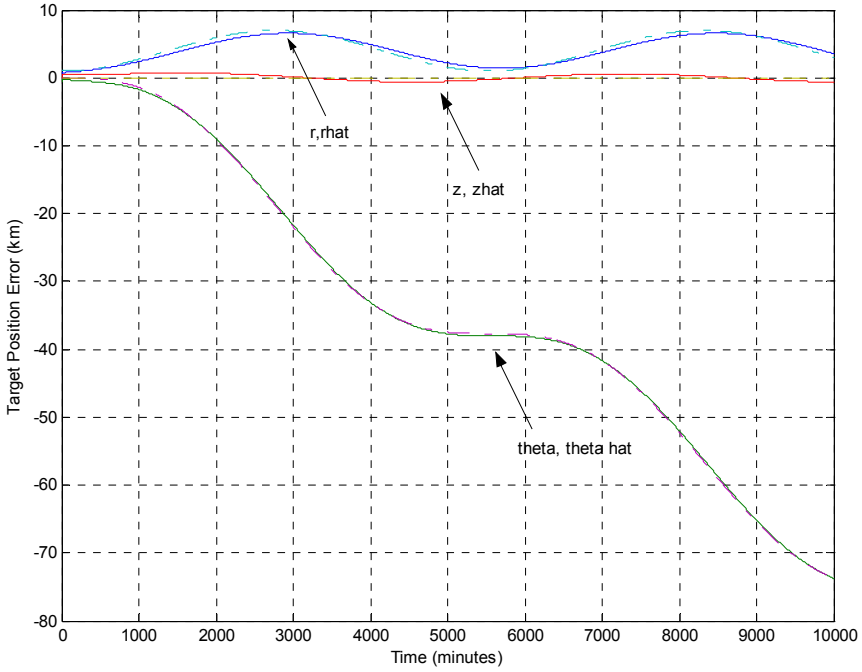

Figure 29. LQE/LSIM Target Position Error with 1 km Initial Error

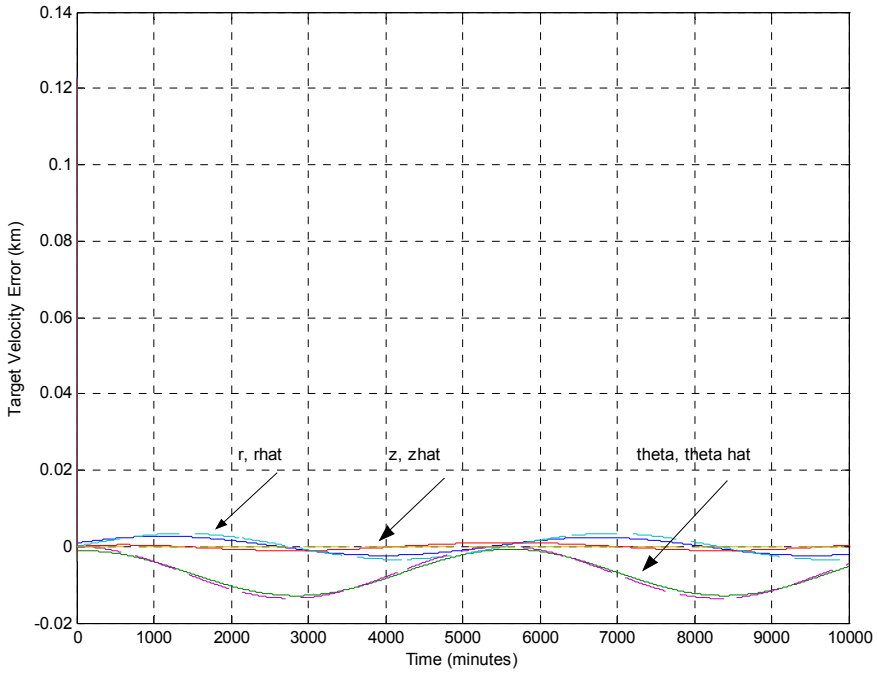

Figure 30. LQE/LSIM Target Velocity Error with 1 km Initial Error

Although the state estimates for the 1 km initial error case also appear to track the truth somewhat well, a closer inspection is required. In this case it is possible to distinguish, graphically, between the truth and estimate. In Figure 31 below, the theta component has been removed to better illustrate the r and z components of the position truth and estimate.

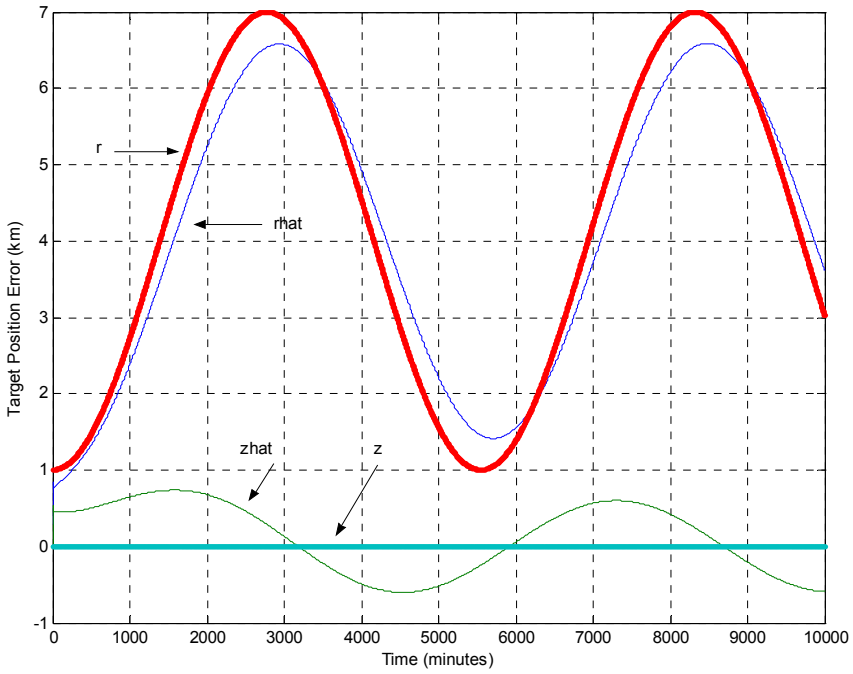

Figure 31. LQE/LSIM Target Position Error with 1 km Initial Error, r and z only

Data taken at the end of the simulation show the total target position error, 841.26 m, and the total velocity error, 1.40 m, are significant. Therefore, the filter does not exhibit the characteristic desired.

Controller/Linear Estimator Integration Results

The simple linear estimator was coupled with a Gain-Scheduling LQR Controller to investigate the system performance. The rendezvous phase focused on remained to be the final 5 km of relative distance between the microsatellite and the target, or OC-3 in Table 2. The first simulation ran open-loop, without microsatellite thrust control, for 200 minutes. The performance tracked against the target truth is provided in Figures 32-33 for reference. The relative distance between the microsatellite and the target truth is

periodic and remains within 20 m of the initial 5 km separation as seem in the fourth subplot of Figure 32.

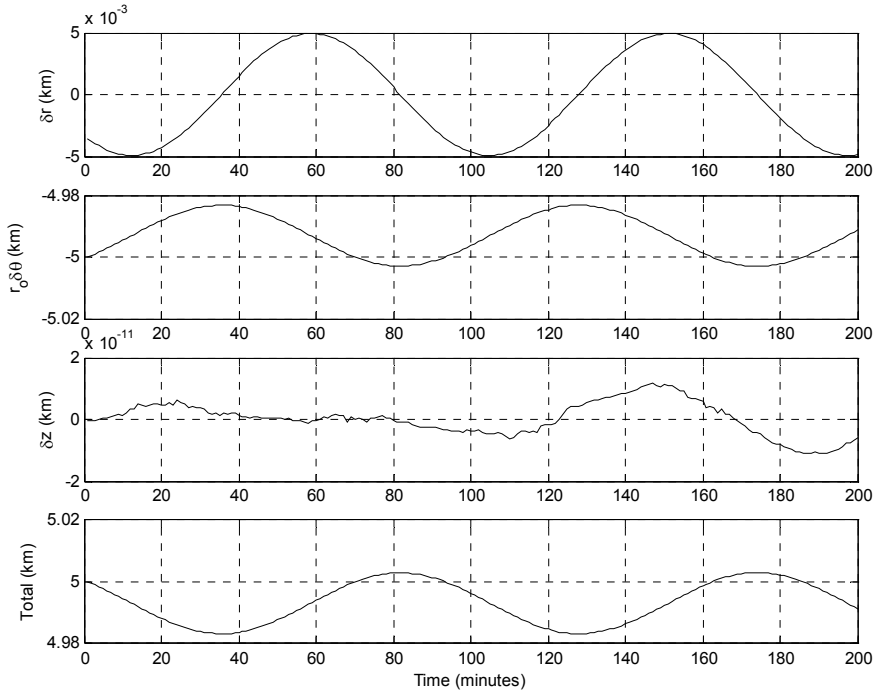

Figure 32. Open-Loop LQR/LQE - Target Truth, Perfect Initial Estimate

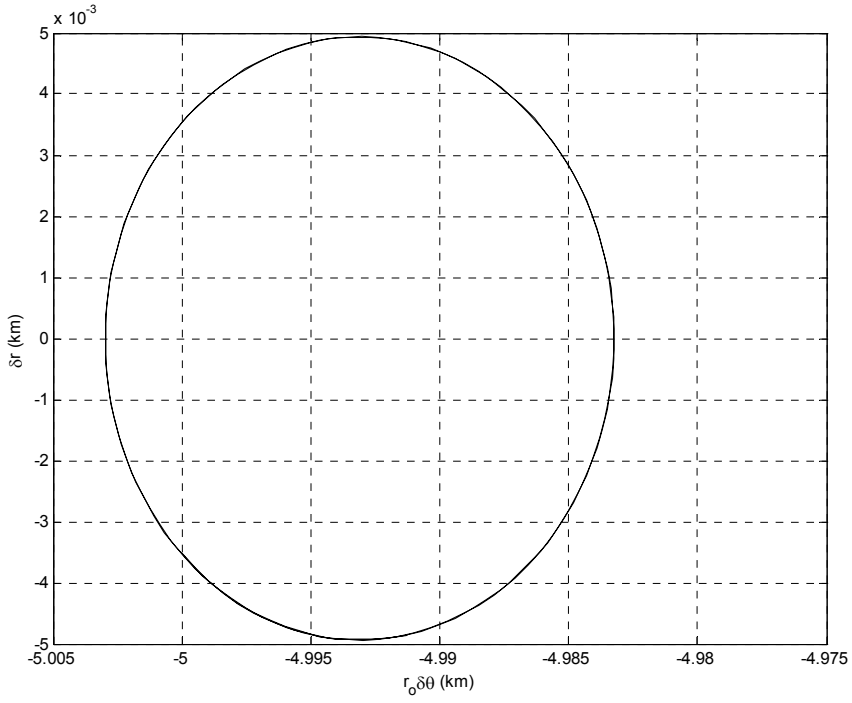

Figure 33. Open-Loop LQR/LQE in $\delta r, r_o\delta\theta$ plane - Target Truth, Perfect Initial Estimate

The performance in Figure 33 above does not track to the origin as the control input is turned off. The resulting open-loop, or "uncontrolled," performance is as expected.

The same performance results, measured against the target estimate, are provided in Figures 34-35. The relative distance between the microsatellite and the target estimate, Figure 34, remains somewhat periodic but is more complex than the perfect initial estimate case shown in Figure 32. The position of the microsatellite relative to the target estimate captured in the $\delta r, r_o\delta\theta$ plane and shown in Figure 35 is far from ideal. It depicts how the microsatellite has a very difficult time simply following the target estimate in this case.

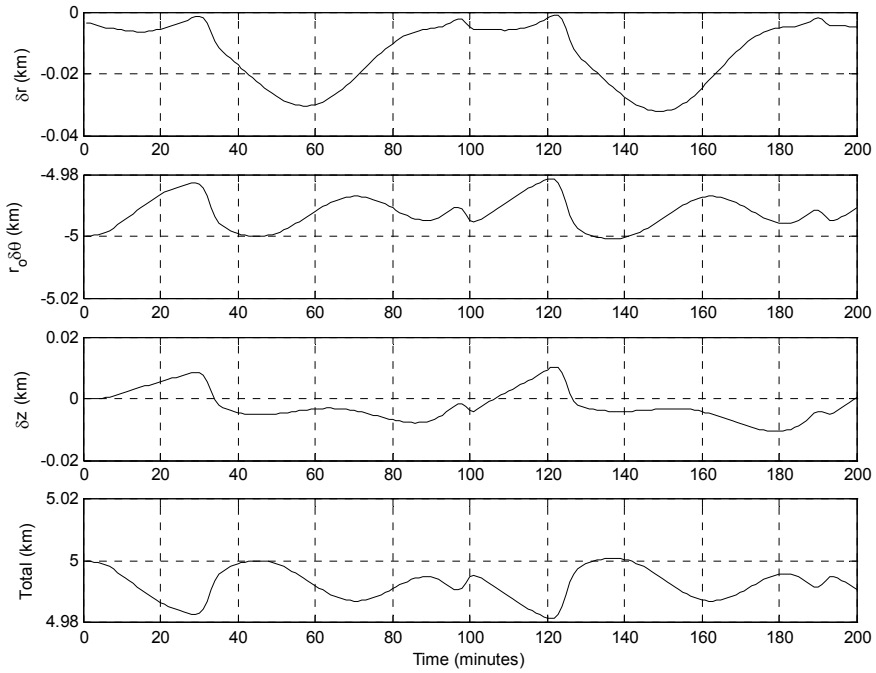

Figure 34. Open-Loop LQR/LQE - Target Estimate, Perfect Initial Estimate

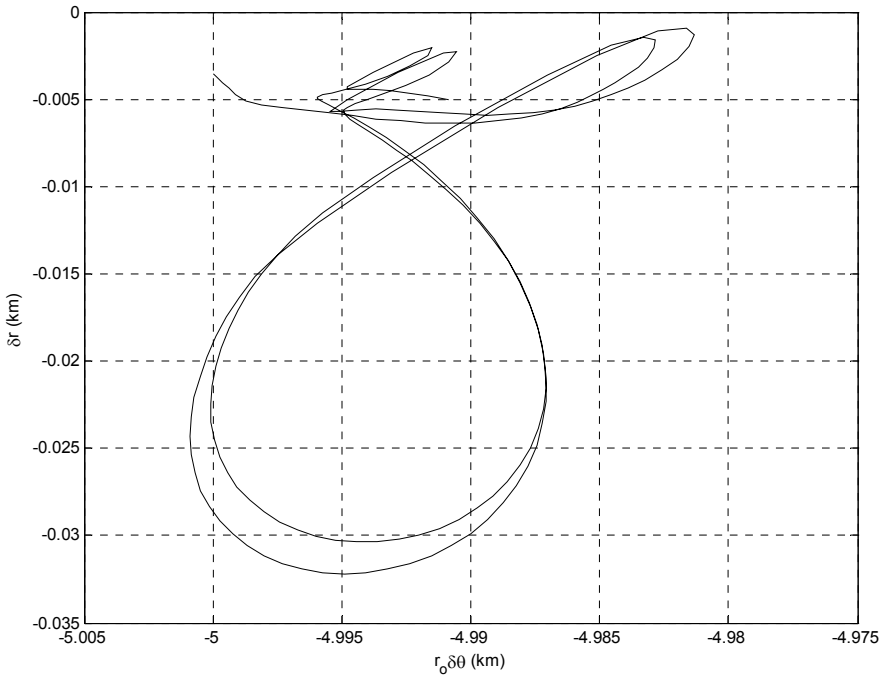

Figure 35. Open-Loop LQR/LQE in $\delta r, r_o \delta\theta$ plane - Target Estimate, Perfect Initial Estimate

This result caused the researcher to take a closer look at the target position error, or the difference between the truth and estimate. The target position error is displayed in Figure 36 for this open-loop case. The fairly periodic waveform of the error has amplitude of approximately 37 m, and period of 92 minutes. The amplitude was found to slightly increase as the simulation time was extended. The target state errors shown in Figure 36 add to the normally periodic open-loop performance shown in Figure 32 producing the open-loop estimate performance in Figure 34.

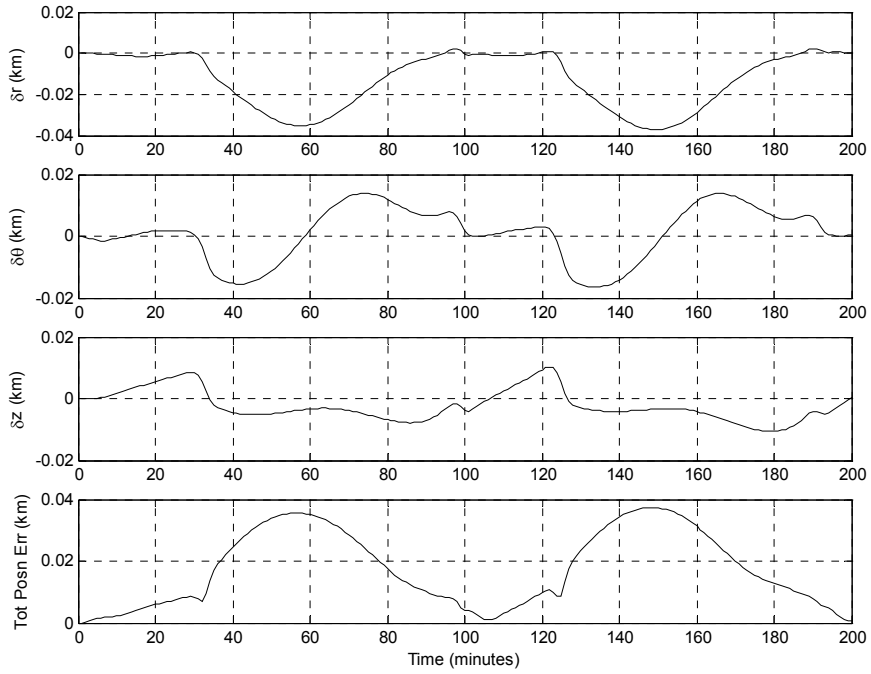

Figure 36. Target Position Error, Perfect Initial Estimate

To illustrate how the estimate error can cause significant difficulties to the rendezvous problem, the loop was closed invoking microsatellite control based on the current target estimate. The simulation again began with a perfect initial estimate for easy comparison to the open-loop performance above. The results are given in Figures 37-38 below. The controller/estimator developed achieves rendezvous to the target in 204 minutes, using 9.36 m/s ΔV. It is important to recall this simulation began with the microsatellite trailing the target from only 5 km and a perfect initial estimate of the target state. Therefore, results should not be directly compared to those by Tschirhart outlined in Chapter II, but represent only the final rendezvous phase studied.

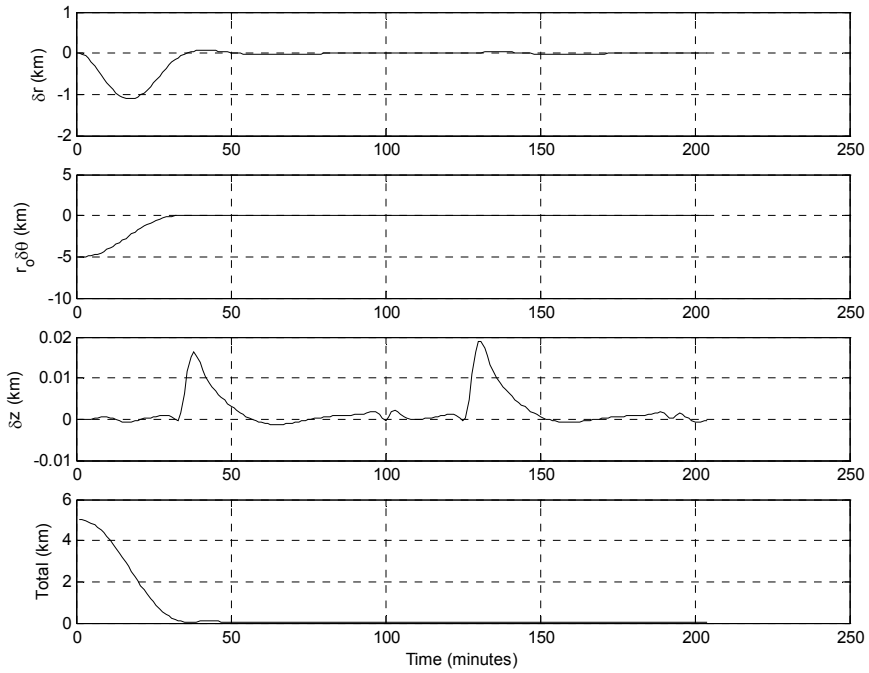

Figure 37. Closed-Loop LQR/LQE - Target Estimate, Perfect Initial Estimate

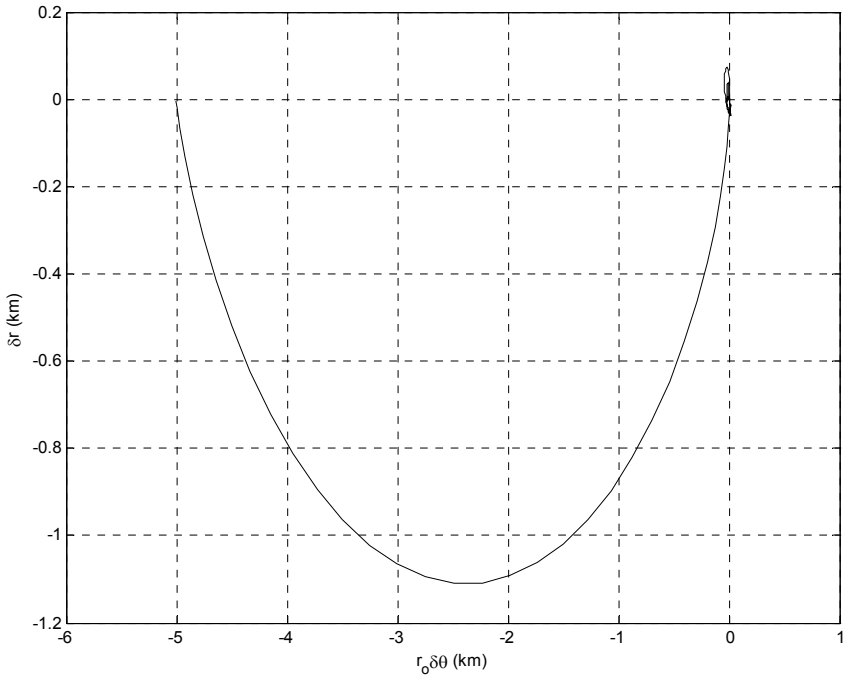

Figure 38. Closed-Loop LQR/LQE in $\delta r, r_o \delta\theta$ plane - Target Estimate, Perfect Initial Estimate

The next task was to include some initial uncertainty in the target estimate. The goal was to demonstrate if the microsatellite could still rendezvous to the target starting with a 1 km target position error. After running the simulation for 1000 minutes, however, the minimum relative distance was never less than 59 m. An initial error of 100 m led to a minimum relative distance of 3.6 m, still greater than the required 1 m rendezvous specification. Rendezvous was achieved, from 5 km out, in 481 minutes, using 12.39 m/s ΔV, beginning with a 10 m target position error. Although this does not represent an achievable initial error, it does help characterize the integrated

controller/estimator performance. The results for this final case are shown in Figures 39-40.

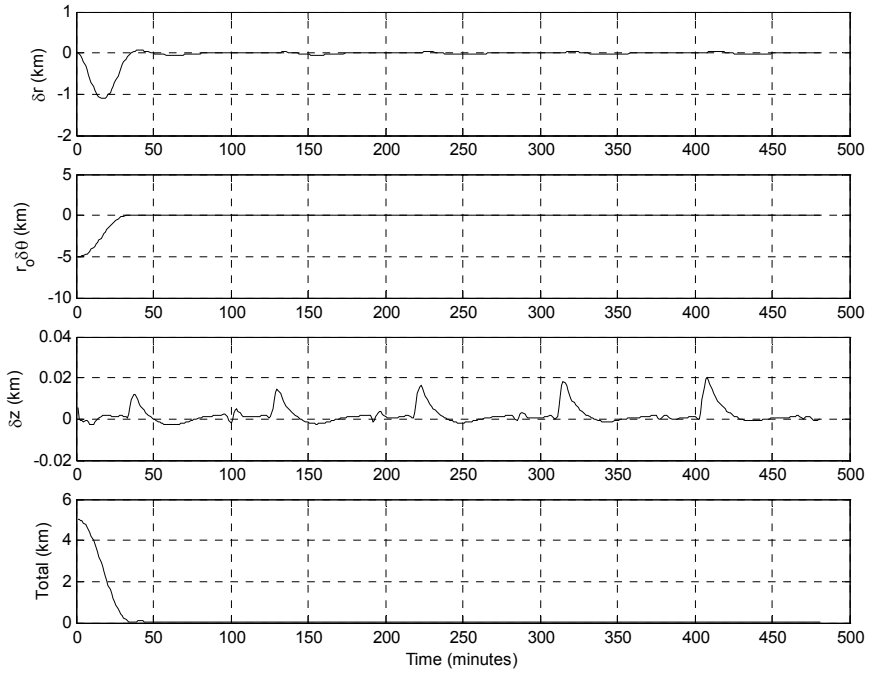

Figure 39. Closed-Loop LQR/LQE - Target Estimate, 10 m Initial Error

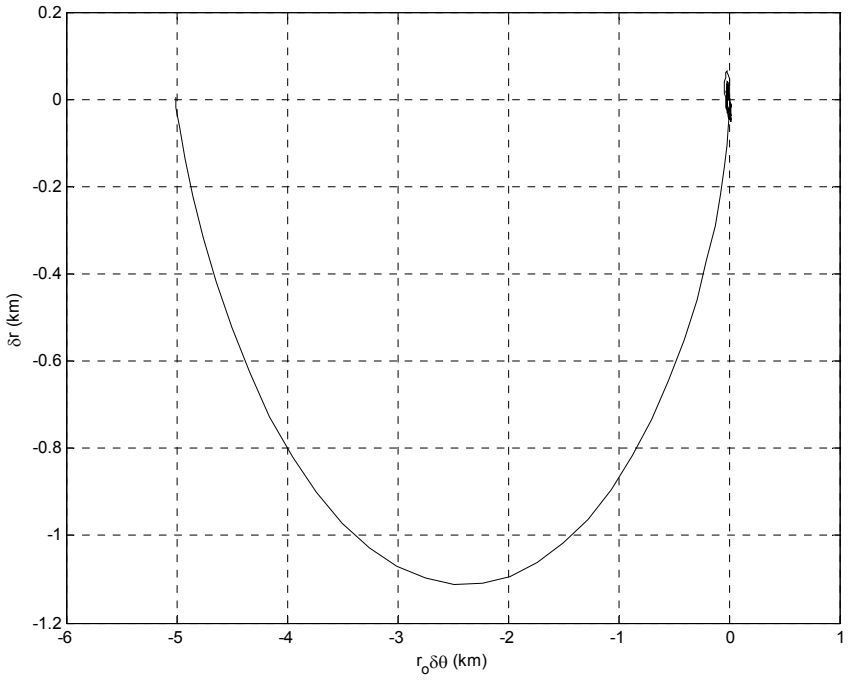

Figure 40. Closed-Loop LQR/LQE in $\delta r, r_o \delta\theta$ plane - Target Estimate, 10 m Initial Error

The conclusion of integrating a linear filter with a Gain-Scheduled LQR controller is that it is not good enough to solve the rendezvous problem. It only works for a nearly perfect model and initial guess. The main obstacle encountered is that a linear filter cannot provide a good enough estimate given the anticipated initial target error.

Nonlinear Filter

The on-orbit Non-linear Least Squares (NLS) estimator developed by Foster, which follows the seven step process outlined in Chapter III, was used as a starting point for this element of the evaluation. The NLS filter was first modified and then characterized to understand the basic performance before integrating with a controller. A

key measure of filter performance is the residual term, or difference between measured and predicted observation values as given in Equation 26.

An open-loop simulation containing 200 observations, separated by one minute each, converged on an estimate after seven filter iterations. The initial estimate included a 1 km position error. The data plot in Figure 41 displays the residual values by iteration. Subsequent iterations provide residuals significantly better than the previous, but it can be difficult to tell the difference graphically. The first iteration was removed in generating Figure 41 to better show the remaining six. It is clear that iterations three through seven are significantly better than iteration two. Likewise, removing iteration two reveals that four through seven are significantly better than three.

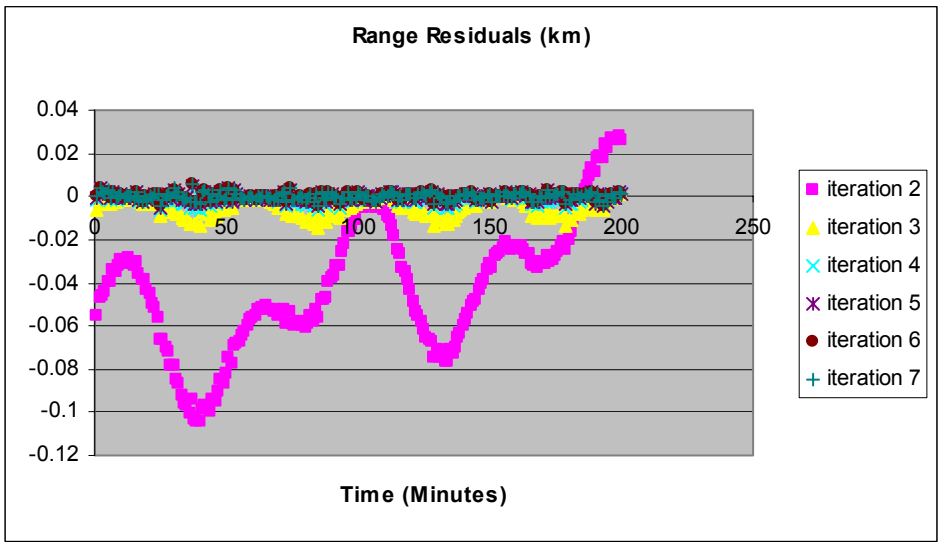

Figure 41. NLS Filter Residuals – Last Six Iterations

The residual values for just the final iteration, in Figure 42, are nicely distributed around zero and captured within +/- 6 m.

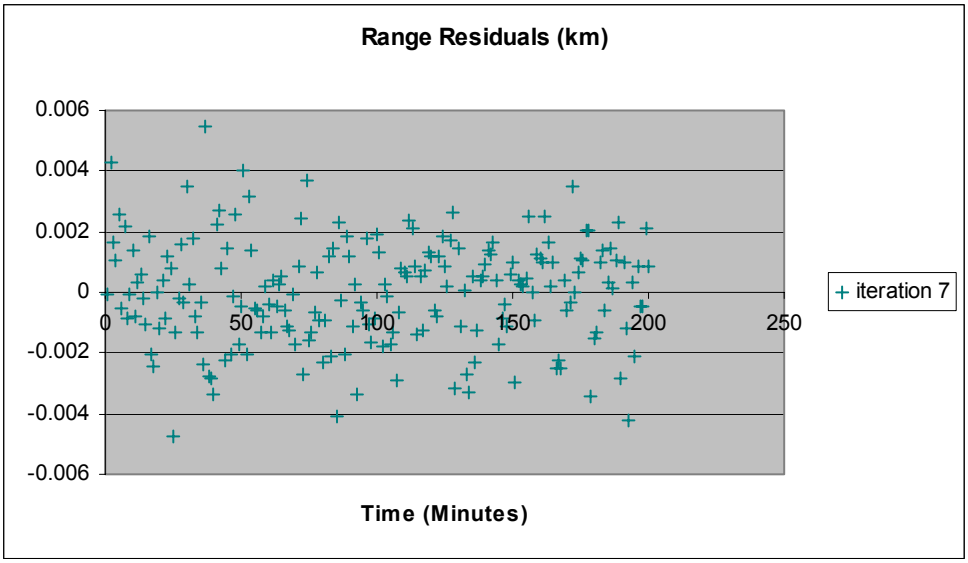

Figure 42. NLS Filter Residuals – Final Iteration

The resulting range residuals provide some confidence the filter is operating as desired. The target position error after the 200 minute simulation is also of great interest, as the filter-provided estimate is the input to the controller. The position error generated, by iteration, is shown in Figure 43. The initial 1 km error data point, iteration 0, has been removed from the chart for clarity.

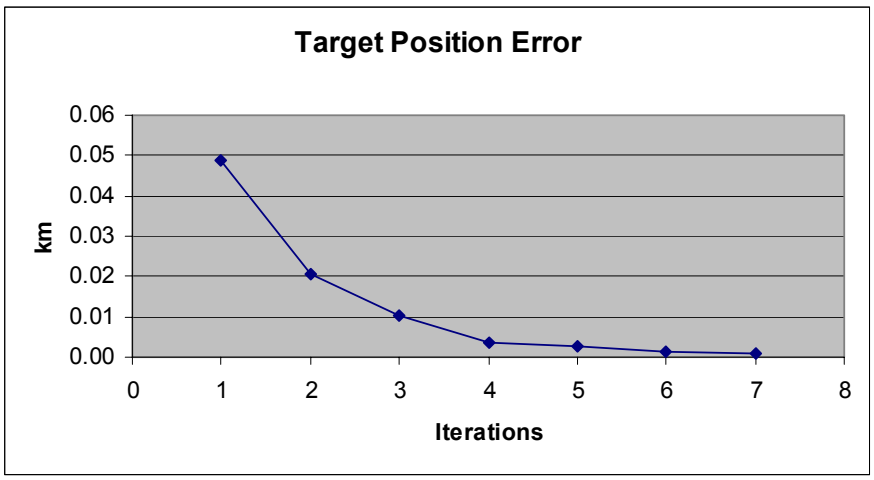

Figure 43. NLS Target Position Errors

After the first iteration, the error is reduced from 1 km to 46.48 m. When convergence is achieved, after seven iterations, the error has been decreased to 1.06 m.

Nominal open-loop filter performance has been assessed to be very good. When the filter has converged on an estimate, both the range residuals and target position error are small, as desired. The next activity was to introduce microsatellite thrust control to rendezvous with the target.

Controller/Nonlinear Estimator Integration Results

The modified NLS estimator characterized above was coupled with a Gain-Scheduling LQR controller to evaluate the potential for closed-loop control from a poor initial estimate. The top-level subsystem architecture was developed based on the algorithm functions and is shown in Figure 44 below.

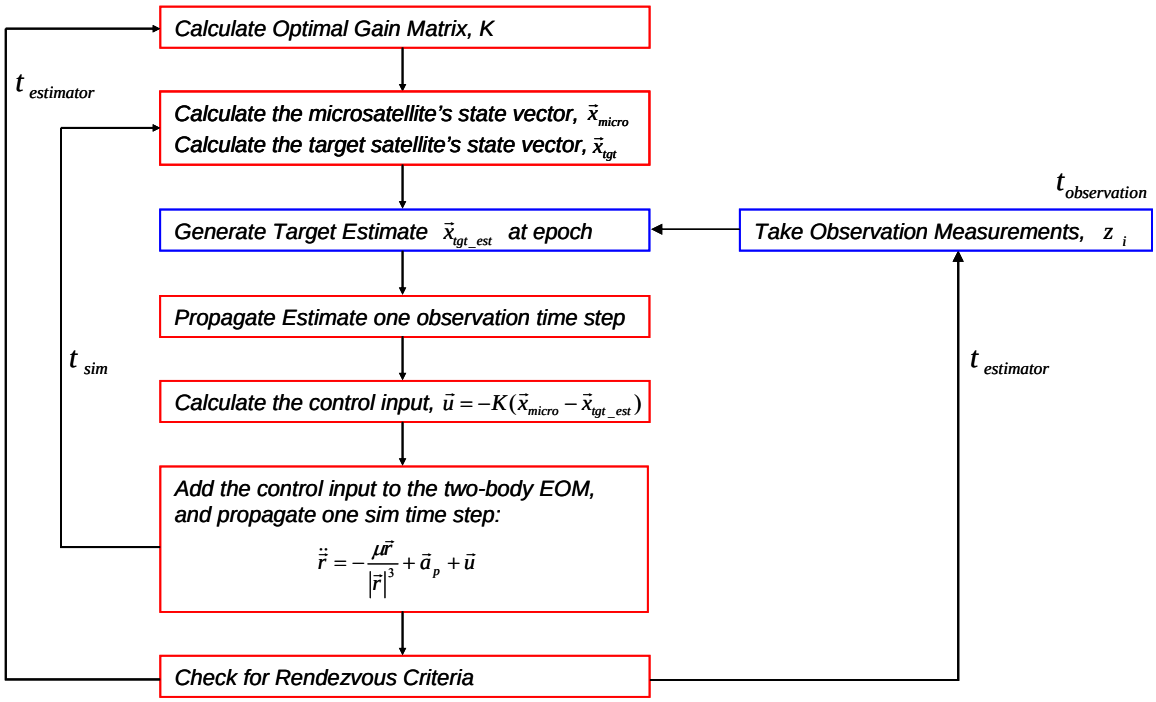

Figure 44. GN&C Algorithm Architecture

Four separate time steps were needed for the simulation. A controller time step, $t_{control}$, an estimator time step, $t_{estimator}$, an observation time step, $t_{observation}$, and a simulation time, t_{sim}. Table 4 below describes the use of each time step. The controller and estimator time steps were set equal to eliminate the need for added complexity to the controller algorithm.

Table 4. Simulation Time Step Definitions

Time Step	Definition
Controller	Time between thrust control updates
Estimatator	Time between estimate updates
Observation	Time between measurement observations
Simulation	Time of orbit propagation

The simulation time used for the stand-alone filter characterization above was 200 minutes. The controller in the integrated system cannot wait 200 minutes for a new target estimate, however. The researcher needed to determine how quickly the filter could provide a reasonable estimate to pass to the controller. Times between the baseline controller (for perfect knowledge) with a controller time step of 60 s and the stand-alone filter time of 12000 s were considered. Beginning with the final 5 km rendezvous phase, OC-3 in Table 2, the integrated controller/estimator simulation was run for a single control loop. The resulting target position error is plotted for various controller time steps in Figure 45. Eliminating the first few data points result in a closer view of the remaining runs, as shown in Figure 46.

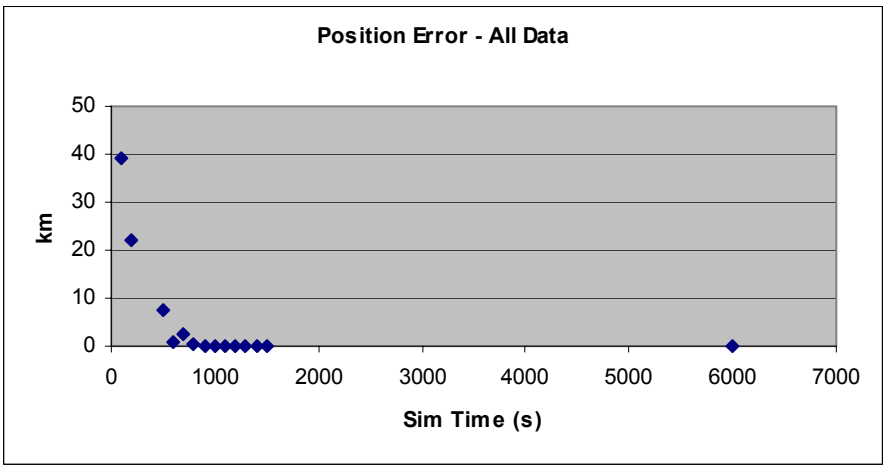

Figure 45. Simulation Time Trade – Target Position Error

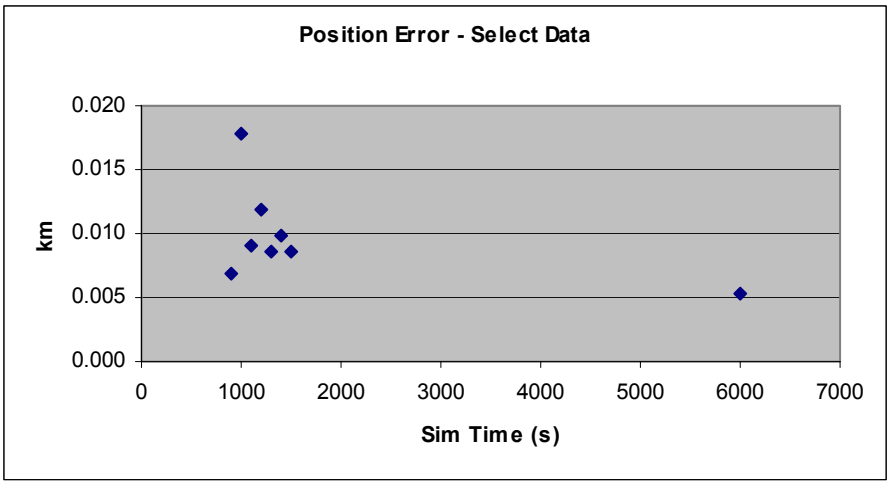

Figure 46. Simulation Time Trade – Target Position Error, Select Data

As the controller controls based on the relative position between the target estimate and microsatellite, a large position error is clearly undesirable. Based on the above, allowing the filter at least 900 s results in a fairly good estimate. Less time yields a useless target estimate.

Studying the relative distance, in addition to the position error, exposes the fact that the controller/estimator time step must be selected carefully. Specifically, a time near 1000 s was found to be most favorable, for a single control loop. This simulation run reduced the relative distance from the initial 5.00 km to 1.04 km. Time steps outside the range of 700-1400 s resulted in the microsatellite drifting further away from the target estimate.

Having identified an initial controller/estimator time step of 1000 s, and an observation time step of 10 s, the integrated system was simulated for multiple control loops in an effort to achieve final rendezvous. The 1000 s time step turned out to be too

large for the controller, however. The performance for the first 20 control loops, 20,000 s of controlled flight, is shown below in Figure 47. The sharp changes are a result of going too long between thrust vector updates in the LQR control. A longer simulation, including more control loops, only results in the relative distance increasing.

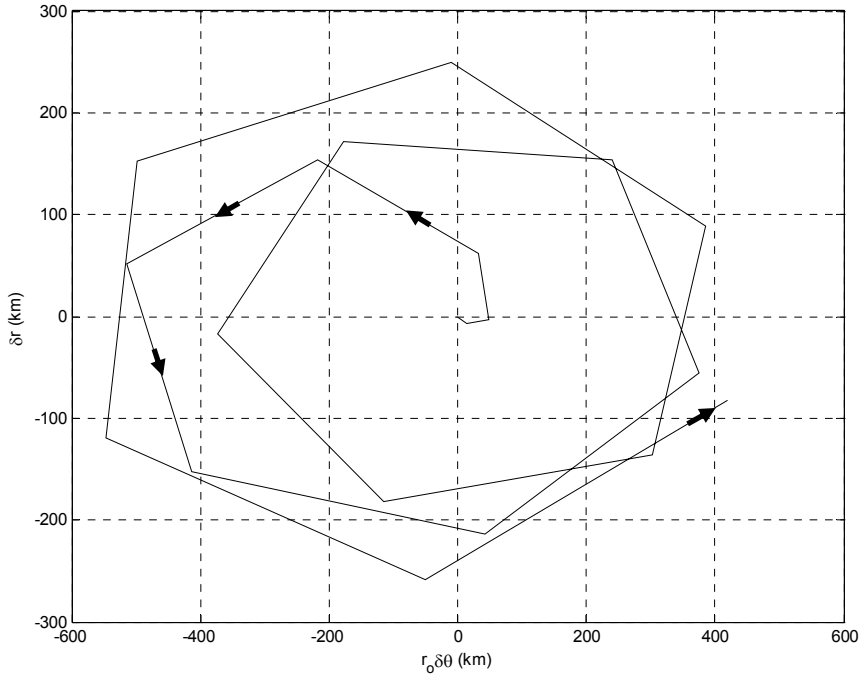

Figure 47. LQR/NLS Performance for $t_{control} = 1000s$, $t_{obs} = 10s$

The target position knowledge begins to significantly degrade after these first 20 control loop iterations, as shown in Figure 48 below. This is the cause for the degenerate performance experienced by running the simulation for longer periods of time.

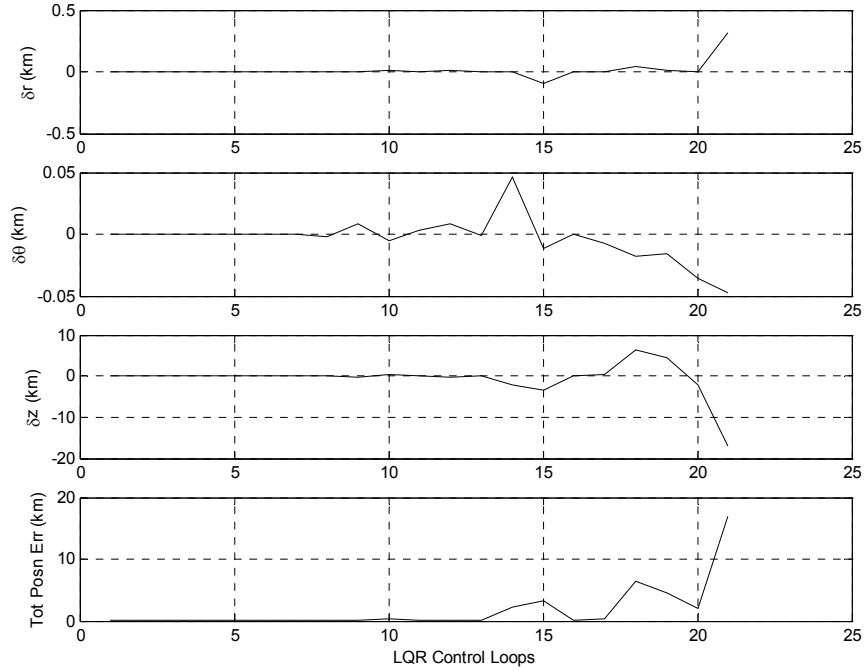

Figure 48. Position Error for $t_{control} = 1000s$, $t_{obs} = 10s$

Backing off on the Control Weighting Matrix, R , was attempted to help smooth out the control vector changes. Specifically, R_{fin} as used in Equations 37 and 38, was increased to 1e13, allowing less control thrust to be applied. Although this did cause a smoother rendezvous approach, the filter was unable to converge on an estimate during the seventh control loop. Figure 49 shows the performance just prior to filter failure. The performance for this case, although still somewhat severe due to the larger controller time step of 1000 s, more closely matches that of the non-gain-scheduled controller assuming perfect knowledge shown in Figure 6. The large time span between control thrust updates has clear negative affect on the ability to meet final rendezvous criteria.

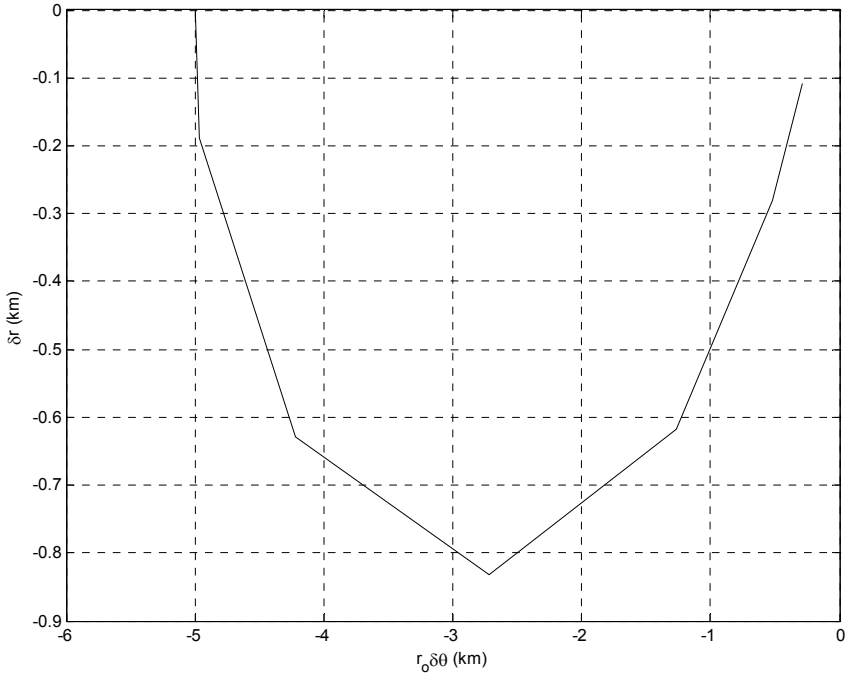

Figure 49. LQR/NLS Improved Performance for $t_{control} = 1000s$, $t_{obs} = 10s$

The other variable control knob, controller/estimator time step, was examined next. The lower bound identified by the simulation time trade study above, 700 s, was used to rerun the simulation. This resulted in filter convergence failure after only a few control iterations, keeping the same 10 s observation time span as above. When the interval was reduced to 1 s, yielding 700 data observations, performance improved. The smoother curve of Figure 50, showing the first 12 control loops, is closer to that desired, but still short of rendezvous. This 140 minute flight from 5 km out brought the microsatellite to within 67 m of the target.

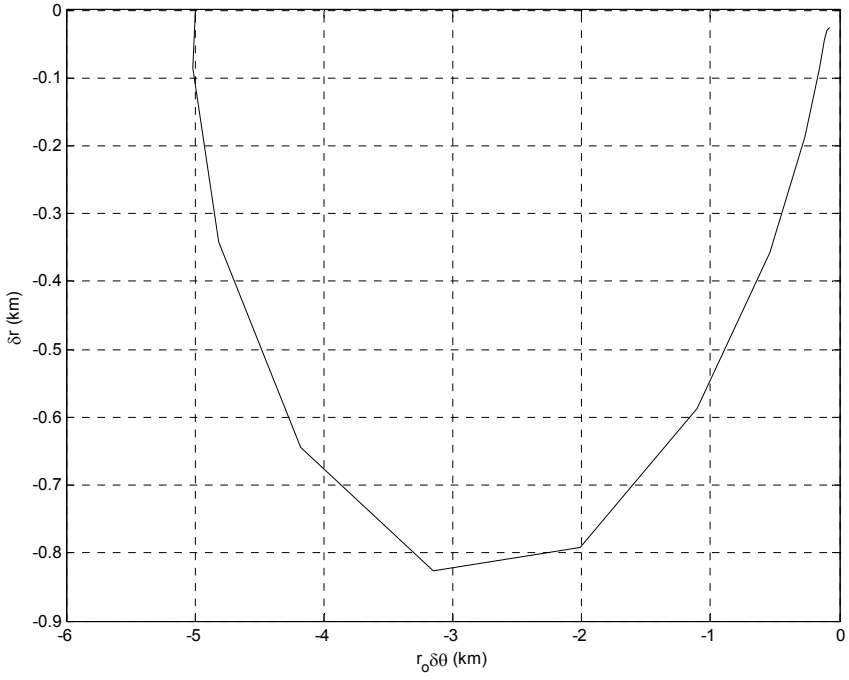

Figure 50. LQR/NLS Improved Performance for $t_{control} = 700\text{s}$, $t_{obs} = 1\text{s}$

Although outside the identified time step range, a run was conducted using 300 s steps for comparison. The results for the first 12 control loops are illustrated in Figure 51. The performance more closely corresponds to a smooth curve, as desired, but breaks down half way to rendezvous as the estimator again fails to converge on an estimate. The above results bound numerous cases attempted, none of which yielded satisfactory performance.

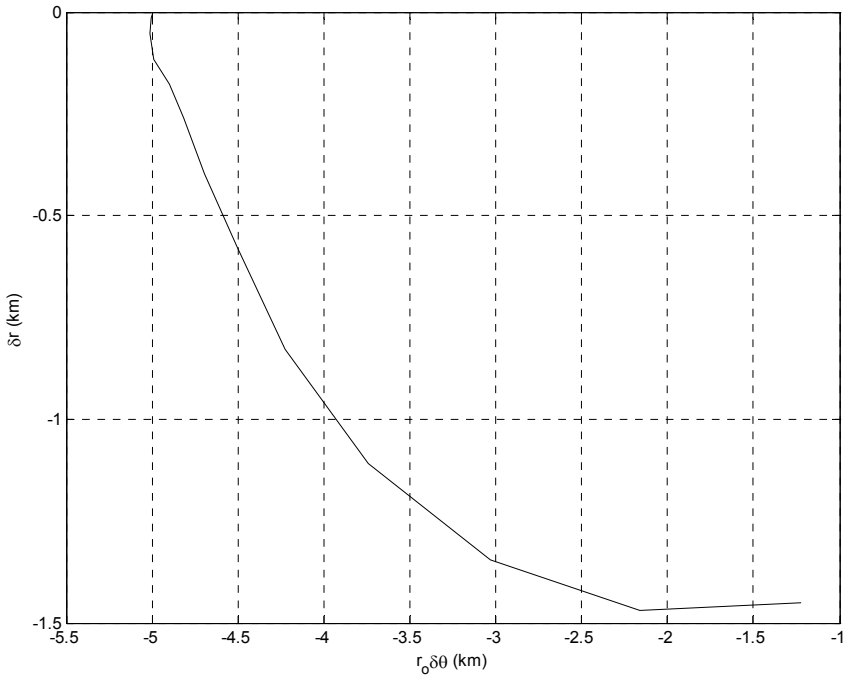

Figure 51. LQR/NLS Improved Performance for $t_{control} = 300s$, $t_{obs} = 1s$

Alternative CONOPS for completing the final rendezvous phase were explored to find a sufficient, even if less elegant, solution. One concept explored was to obtain a good estimate by following the target open-loop, and then quickly controlling without updating the estimate. The system would perform an initial orbit determination using the onboard sensor and then control to that solution without further updates. In this case, the estimate containing a 1 m initial error was simply propagated forward until the catch criteria was met. This scenario resulted in rendezvous to the target estimate in 71 minutes from the 5 km start. The performance is provided in Figure 52. As this case

employs the same small controller time step, 60 s, as the original LQR controller that assumed truth, the performance is very similar to that shown in Figure 6.

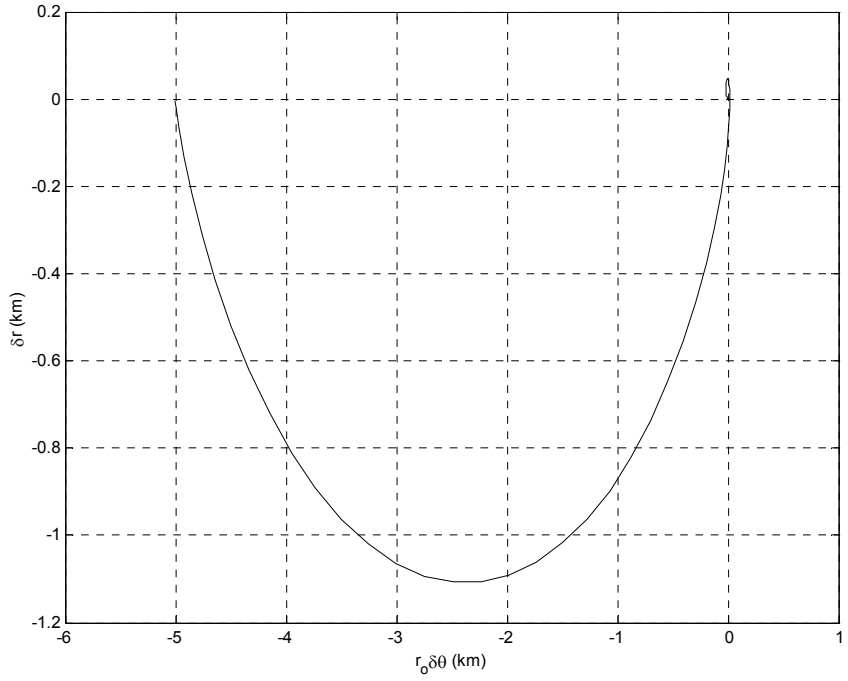

Figure 52. Blind Rendezvous Performance

Although the 1 m relative distance criterion, to the target estimate, was met, the relative distance to the target truth is the important measure. Given a small target position error, the two distances would be very similar. In this case, however, the error built up over the 71 minute simulation resulted in a 12 m relative distance to the truth when the controller believed rendezvous had been achieved.

A further complication with this alternative CONOPS is the lack of robustness. Once perturbations are introduced, such as air drag, it fails to achieve rendezvous even to

the target estimate. The simulation was run, including J2, for 200 minutes resulting in the performance shown in Figure 53.

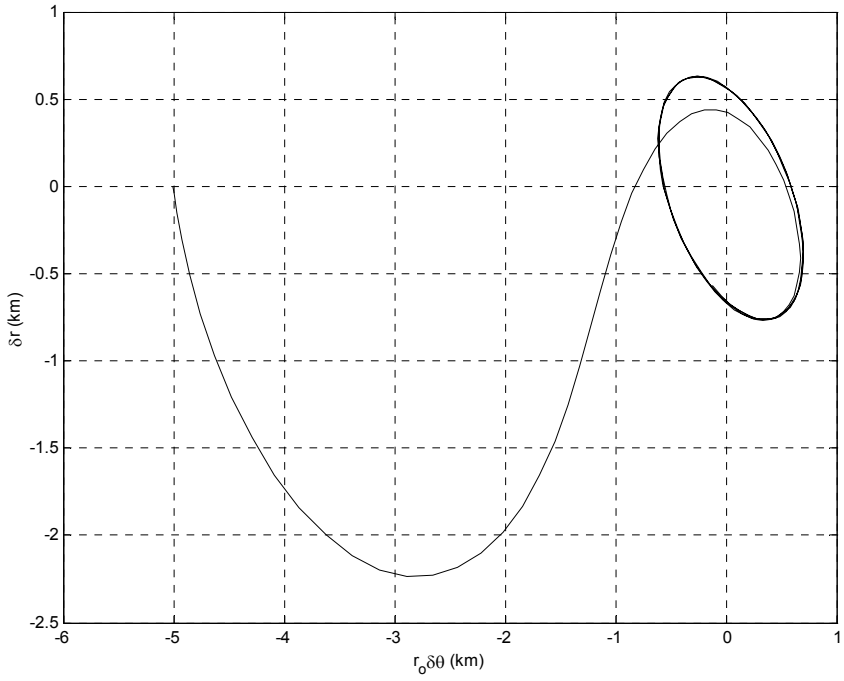

Figure 53. Blind Rendezvous Performance with J2

In this case, the target position error becomes so large; there is no hope of closure. The difference between the estimate and truth continuously increases during the simulation. Figure 54 shows how this error builds up to over 100 m after just 140 minutes.

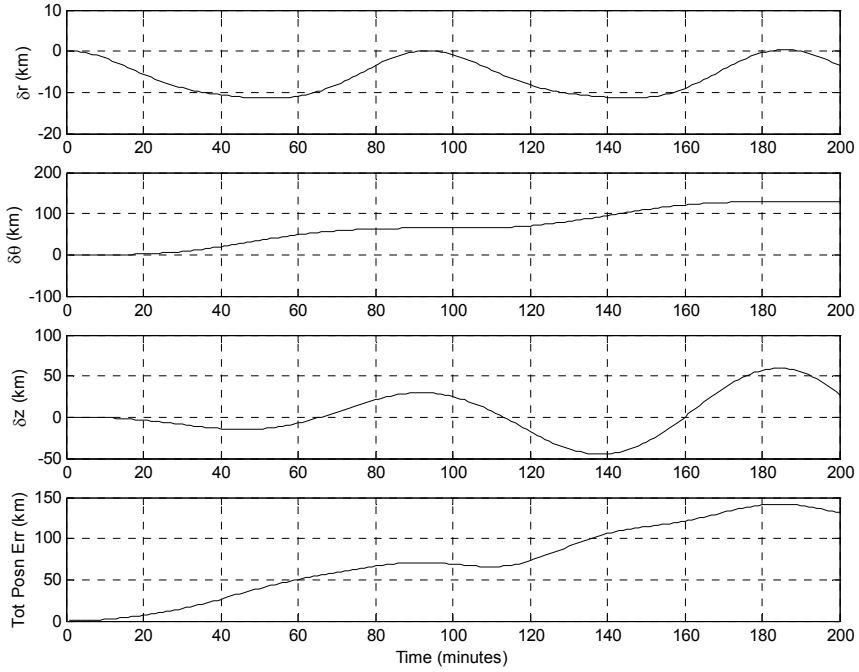

Figure 54. Position Error for Blind Rendezvous with J2

Summary

Front-end Systems Engineering led to a top-level system feasibility, but also exposed GN&C integration complexity. Controller and estimator algorithms have been separately matured from previous work and shown to contain a fair amount of adaptability. As an example, Gain-Scheduling was found to significantly improve upon earlier Linear Quadratic Regulator performance. Difficulty arose, however, when the development of an integrated GN&C subsystem was attempted. It proved to be outside the context of established algorithms and required additional effort to extend.

V. Conclusions and Recommendations

Chapter Overview

This chapter summarizes the feasibility analysis of a microsatellite rendezvous with non-cooperative targets and identifies the technical challenges in doing so. The integration challenges encountered in the GN&C algorithm assimilation provide rich opportunity for future research activities.

Conclusions of Research

The results of this research underscore the difficulty in developing an integrated GN&C system for a non-cooperative rendezvous. The competing demands of the controller and estimator components prove too much for simple algorithms to overcome. The suite of continuous nonlinear control, linearized dynamics, and non-linear measurement conditions need to be fully accounted for in the integrated solution. The NLS estimator developed for this research, however, has no means to include the continuously changing measurements. This causes error to build up in the target estimate between updates, greatly hindering the process. Although a top-level system architecture was developed, the technical complexity involved requires more sophisticated methods to solve.

Recommendations for Future Research

As political economist Thomas Schelling has pointed out, "There is a tendency in our planning to confuse the unfamiliar with the improbable. The contingency we have not considered looks strange; what looks strange is thought improbable; what is

improbable need not be considered seriously." Surprise is most often not a lack of warning, but the result of a tendency to dismiss as reckless what we consider improbable (Commission to Assess US National Security Space Management & Organization, 2001). Although the conclusion of this research points to a low level of feasibility, given the scope, it should not be considered unfamiliar or improbable.

As future work, the control and estimation algorithms used need to be further tailored to incorporate all physical conditions involved in the rendezvous problem. Taking everything into account may reveal a feasible solution. More development time is needed to mature the software.

Although past research indicate an impulsive thrust solution does not work, even given perfect knowledge of the target, it seems additional study may reveal a viable product. As it was very difficult to integrate a continuous thrust controller with an estimator in this work, the impulsive controller should be revisited. Specifically, coupling a CW controller with a modified NLS filter could present interesting results. Optimal sequential processing with noise statistics assumed should be investigated.

Once a technical solution is found, the systems engineering work should be expanded to include a more formal evaluation. A full system architecture should first be developed followed by more rigorous evaluation techniques. Executable models could be developed upon which to base a quantitative assessment of system feasibility. A detailed GN&C subsystem feasibility study should be conducted to explore hardware/software integration challenges, followed by a full system study to look at subsystem integration issues.

Appendix A – Main LQR Code

```
%==========================================================
%
%  MAIN LQR CODE
%
%  Allen Toso - 7 Feb 04
%
%  Orbital Rendezvous With a Non-Cooperative Target
%
%  Original code provided by Troy Tschirhart (4 Mar 03)
%  Code modified to incorporate Estimator and focus on final 5 km approach
%
%==========================================================

%==========================================================
%
%  This program uses the following function files which must be on the current path:
%
%  atmosphere.m      calculate atmospheric density at the given altitude
%  CalcInit.m        calculate the initial conditions for the run
%  Do_Plots          plot the results
%  LQR_Rend          accomplish lqr rendezvous manuever
%  propagate.m       propagator
%  posvel.m          set up the differential equation for the propagator
%  ijk2pqw.m         transform r,v from ijk frame to pqw frame
%  pqw2ijk.m         transform r,v from pqw frame to ijk frame
%  rtz2pqw.m         transform r,v from rtz frame to pqw frame
%  rv2coe.m          calculate coe for the given r,v
%  coe2rv.m          calculate r,v for the given coe
%
%==========================================================

%==========================================================
%  Clear Variables and Set Format Options
%==========================================================

clear
format long g
format compact

%==========================================================
%  Print a banner to separate results
%  Start the timer (used at the end to determine how long the run took)
```

```
%=================================================================

('=================================================================')

tic

%=================================================================
%  Set Selectable Variable Values
%=================================================================

%-----------------------------------------------------------------------------------------------
%  The target's actual initial COEs
%-----------------------------------------------------------------------------------------------

coe_tgt_act(1) = 6.772888912204840e+003;        % km            a
coe_tgt_act(2) = 9.887713549825913e-004;        % dimensionless     e
coe_tgt_act(3) = 0.79736386485827;              % radians       nu
coe_tgt_act(4) = 0.90757990078380;              % radians       i
coe_tgt_act(5) = 1.51843760980691;              % radians       cap_omega
coe_tgt_act(6) = 5.59054044657763;              % radians       small_omega
coe_tgt_act(7) = 0.0;                           % seconds       time since perigee

%-----------------------------------------------------------------------------------------------
%  Set initial micro offset from the target
%-----------------------------------------------------------------------------------------------

delr = 0;                       % kilometers (delta_r)
dist = -5;                      % kilometers arclength (ro*delta_theta)
delz = 0;                       % kilometers (delta_z)

%-----------------------------------------------------------------------------------------------
%  Set the acceptable relative distance and velocity for a successful rendezvous
%-----------------------------------------------------------------------------------------------

catchdis = 0.001;       % kilometers (1m) - Phase 2 (O/L), Phase 3 (C/L)
catchvel = 0.00001;     % kilometers/second (1cm/s) - Phase 2

timestep = 1000;        % used only to determine delta_thrust in LQR, based on filter
                        % (seconds)

%-----------------------------------------------------------------------------------------------
%  Specify values for the state weighting matrix, Q
%  and the control weighting matrix, R
%  Note:  Q_mag increases => faster movement from initial to desired states
%  R_mag increases => lower control usage
```

```
%-------------------------------------------------------------------------------------------

Q_mag = 1;
R_fin = 1e13;

%-------------------------------------------------------------------------------------------
%  Set perturbation (J2) options (Note: "1" = option selected; "0" = option not selected)
%-------------------------------------------------------------------------------------------

pert =0;

%-------------------------------------------------------------------------------------------
%  Set drag options and values (Note: "1" = option selected; "0" = option not selected)
%-------------------------------------------------------------------------------------------

dragtgt = 0;
cd_tgt = 2.2;                                   % Drag coefficient of the target
a_tgt = 3.5*1.2/(1000^2);                       % Area of the target (km^2)
m_tgt = 725;                                    % Mass of the target
cdamtgt = dragtgt * (cd_tgt * a_tgt) / m_tgt; % Calculate the target's cdam value

%-------------------------------------------------------------------------------------------

dragmic = 0;
cd_mic = 3;                                     % Drag coefficient of the micro
a_mic = 1.5/(1000^2);                           % Area of the micro (km^2)
m_mic = 100;                                    % Mass of the micro
cdammic = dragmic * (cd_mic * a_mic) / m_mic;    % Calculate the micro's cdam value

%-------------------------------------------------------------------------------------------
%  Set plot options (Note: "1" = option selected; "0" = option not selected)
%-------------------------------------------------------------------------------------------

prdijk = 0;    % Plot relative distance in the inertial (ijk) frame
prdrtz = 1;    % Plot relative distance in the relative (rtz) frame
prdroto = 1;   % Plot relative distance in the relative plane (delta_r, ro*delta_theta)

%===========================================================================
%  Initialize variable values
%===========================================================================

delta_v_accum = 0;          % initialize delta-V to zero

%===========================================================================
%  Calculate Initial Values
```

```
%  1.  Target's initial position and velocity
%  2.  Micro's initial position and velocity
%==========================================================================

CalcInit

%==========================================================================
%  Accomplish Linear Quadratic Regulator Rendezvous
%==========================================================================

LQR_Rend

%==========================================================================
%  Print Output Values
%==========================================================================

delta_r = delr
ro_delta_theta = dist
delta_z = delz

pert
dragtgt
dragmic
pt
timestep
Q_mag
R_mag
delta_v_accum
final_vel = vel_now
final_dist = dist_now

%==========================================================================
%  Draw Desired Plots
%==========================================================================

Do_Plots

%==========================================================================
%  End of Program
%==========================================================================

run_time = toc
```

Appendix B – Linear Estimator Code

```
%================================================================
%
%  STAND ALONE LQE_LSIM ESTIMATOR (Linear Estimator)
%
%  Allen Toso - 2 Dec 03
%
%  Orbital Rendezvous With a Non-Cooperative Target
%  Uses Range, Az, El to obtain an estimate for the target state
%
%  [L, P, E] = LQE(A,G,C,Q,R)
%
%  A = Plant (System)
%  G = something small
%  C = Observation Geometry Matrix - Range Vector Range, Az, El)
%  Q = Strength of Process Noise, set to zero
%  R = Strength of Measurement Noise
%
% [y,x] = LSIM(A,B,C,D,u,t,x_tgt')
%
% [y_hat, x_hat] = LSIM(A_ob,L,C,D,y,t,x_tgt_hat')
%
%================================================================

% Initial input %
clear
format long g
format compact

x_tgt =     [0  1  0  0  0  0]                    % detla r only

r_tgt_rel(1) = x_tgt(2);
r_tgt_rel(2) = x_tgt(4);
r_tgt_rel(3) = x_tgt(6)

v_tgt_rel(1) = x_tgt(1);
v_tgt_rel(2) = x_tgt(3);
v_tgt_rel(3) = x_tgt(5);


x_tgt_hat = x_tgt;

pos_error = .70710678;                    % amounts to 1 km position error
```

```
r_tgt_hat_rel(1) = x_tgt_hat(2) - pos_error;
r_tgt_hat_rel(2) = x_tgt_hat(4) - pos_error;
r_tgt_hat_rel(3) = x_tgt_hat(6)

v_tgt_hat_rel(1) = x_tgt_hat(1);
v_tgt_hat_rel(2) = x_tgt_hat(3);
v_tgt_hat_rel(3) = x_tgt_hat(5);

x_tgt_hat(2) = r_tgt_hat_rel(1);
x_tgt_hat(4) = r_tgt_hat_rel(2);
x_tgt_hat(6) = r_tgt_hat_rel(3)


%=========================================================================
% Calc A
%=========================================================================


U = 398601;         % km^3/sec^2

coe_tgt_act(1) = 6.772888912204840e+003; % a, km
coe_ref = coe_tgt_act;                   % Start with target's initial COEs

n=sqrt(U/coe_ref(1)^3);

A=[ 0    3*n^2  2*n  0  0   0;
    1    0      0    0  0   0;
   -2*n  0      0    0  0   0;
    0    0      1    0  0   0;
    0    0      0    0  0  -n^2;
    0    0      0    0  1   0];


%=========================================================================
% Calc C
%=========================================================================

% Calc the norm of target state, x_tgt, in rtz, in km

% Relative position vector (3 x 1) (range) in rtz coordinates
% to the target satellite.
range_vector = r_tgt_hat_rel;

% Magnitude of the range vector in rtz, in km
```

```
range = norm(range_vector);

% C = Observation Geometry Matrix - Range Vector Range, Az, El)
% Initialize C to zeros first then build up needed components
C = zeros(3,6);

% C(1,1), C(2,1), C(3,1) = 0

% C(1,2), C(2,2), C(3,2):
C(1,2) = range_vector(1) / range;
C(2,2) = (-range_vector(2)/range_vector(1)^2) / (1 +
(range_vector(2)/range_vector(1))^2);

C3_2_top = (-range_vector(1)*range_vector(3)) / ((range_vector(1)^2 +
range_vector(2)^2)^(3/2));
C3_2_bottom = 1 + (range_vector(3)^2) / (range_vector(1)^2 + range_vector(2)^2);
C(3,2) = C3_2_top / C3_2_bottom;

% C(1,3), C(2,3), C(3,3) = 0

% C(1,4), C(2,4), C(3,4):
C(1,4) = range_vector(2) / range;
C(2,4) = (1/range_vector(1)) / (1 + (range_vector(2)/range_vector(1))^2);

C3_4_top = (-range_vector(2)*range_vector(3)) / ((range_vector(1)^2 +
range_vector(2)^2)^(3/2));
C3_4_bottom = 1 + (range_vector(3)^2) / (range_vector(1)^2 + range_vector(2)^2);
C(3,4) = C3_4_top / C3_4_bottom;

% C(1,5), C(2,5), C(3,5) = 0

% C(1,6), C(2,6), C(3,6):
C(1,6) = range_vector(3) / range;
C(2,6) = 0;

C3_6_top = 1 / ((range_vector(1)^2 + range_vector(2)^2)^(1/2));
C3_6_bottom = 1 + (range_vector(3)^2) / (range_vector(1)^2 + range_vector(2)^2);
C(3,6) = C3_6_top / C3_6_bottom;

%=================================================================
% Calc L, estimator gain matrix
%=================================================================

%  [L, P, E] = LQE(A,G,C,Q,R)
```

```
%  A = Plant (System)

%  G = something small

G = [1 1 1;
    1 1 1;
    1 1 1;
    1 1 1;
    1 1 1;
    1 1 1];

% Form Q, the process noise matrix nonzero - two orders of magnitude smaller than R,
allow R to dominate
% Q(1,1) = 0.0002^2; - Reference: Foster's obser.m

Q = zeros(3,3);

Q(1,1) = 0.00000004;
Q(2,2) = 0.00000004;
Q(3,3) = 0.00000004;

% R = Strength of Measurement Noise
% Form R, the instrumental covariance matrix
% R(1,1) = 0.002^2;     Instrumentation sigma squared ( 2 meters = 0.002 km)

R = zeros(2,2);

R(1,1) = 0.000004;
R(2,2) = 0.000004;
R(3,3) = 0.000004;


[L,P,E] = lqe(A,G,C,Q,R);


%=============================================================
% Call LSIM
%=============================================================

B = [ 0;
     0;
     0;
     0;
     0;
     0];
```

```
D = 0;

A_ob = A-L*C;

t = [0:1:10000]';

u = 0*t;

[y,x] = lsim(A,B,C,D,u,t,x_tgt');

[y_hat, x_hat] = lsim(A_ob,L,C,D,y,t,x_tgt_hat');


%==========================================================================
% Plot results
%==========================================================================

% Parse x
r_tgt_plot(:,1) = x(:,2);
r_tgt_plot(:,2) = x(:,4);
r_tgt_plot(:,3) = x(:,6);

v_tgt_plot(:,1) = x(:,1);
v_tgt_plot(:,2) = x(:,3);
v_tgt_plot(:,3) = x(:,5);

% Parse x_hat
r_tgt_hat_plot(:,1) = x_hat(:,2);
r_tgt_hat_plot(:,2) = x_hat(:,4);
r_tgt_hat_plot(:,3) = x_hat(:,6);

v_tgt_hat_plot(:,1) = x_hat(:,1);
v_tgt_hat_plot(:,2) = x_hat(:,3);
v_tgt_hat_plot(:,3) = x_hat(:,5);

figure(1); clf;
plot(t,r_tgt_hat_plot,t,r_tgt_plot,'--'); grid on; ylabel('Target Position Error (km)');
xlabel('Time (minutes)');

figure(2); clf;
plot(t,v_tgt_hat_plot,t,v_tgt_plot,'--'); grid on; ylabel('Target Velocity Error (km)');
xlabel('Time (minutes)');
```

```
%=================================================================
% Check target position and velocity errors
%=================================================================

x_tgt_next = x(10000,:)

r_tgt_rel(1) = x_tgt_next(2);
r_tgt_rel(2) = x_tgt_next(4);
r_tgt_rel(3) = x_tgt_next(6)

v_tgt_rel(1) = x_tgt_next(1);
v_tgt_rel(2) = x_tgt_next(3);
v_tgt_rel(3) = x_tgt_next(5)


x_tgt_hat_next = x_hat(10000,:)

r_tgt_hat_rel(1) = x_tgt_hat_next(2);
r_tgt_hat_rel(2) = x_tgt_hat_next(4);
r_tgt_hat_rel(3) = x_tgt_hat_next(6)

v_tgt_hat_rel(1) = x_tgt_hat_next(1);
v_tgt_hat_rel(2) = x_tgt_hat_next(3);
v_tgt_hat_rel(3) = x_tgt_hat_next(5)


tgt_posn_error = r_tgt_rel' - r_tgt_hat_rel'

tgt_posn_error = norm(tgt_posn_error)


tgt_vel_error = v_tgt_rel' - v_tgt_hat_rel'

tgt_vel_error = norm(tgt_vel_error)


%=================================================================
% End of Program
%=================================================================
```

Bibliography

"Baby Satellites," European Space Agency website, (24 September 2003). 3 February 2004 http://www.esa.int/export/esaCP/SEMQ5D0P4HD_FeatureWeek_0.html.

Brooks, C.G., J.M. Grimwood, and L.S. Swenson Jr. *Chariots for Apollo: A History of Manned Lunar Spacecraft*. NASA, Washington DC, 1979.

Buede, Dennis M. *The Engineering Design of Systems.* New York: John Wiley & Sons, Inc, 2000.

Cobb, Richard G. Class handout, SENG 765, Robust Control. Graduate School of Engineering and Management, Air Force Institute of Technology, Wright-Patterson AFB OH, April 2003.

Commission to Assess United States National Security Space Management and Organization. Report of the Commission to Assess United States National Security Space Management and Organization. Washington DC, 11 January 2001.

D'Azzo, John J. and Constantine H. Houpis. *Linear Control Systems Analysis & Design (3rd Edition)*. New York: McGraw-Hill Publishing Company, 1988.

Department of Defense. Space Policy. DoD Directive 3100.10. Washington GPO, 9 July 1999.

DoD Architecture Framework Working Group. DoD Architecture Framework (DoDAF) Version 1.0. Final Draft, 30 August 2003.

Department of the Air Force. Space Operations. Air Force Doctrine Document 2-2. Washington: HQ USAF, 21 November 2001.

Foster, Brian L. *Orbit Determination for a Microsatellite Rendezvous with a Noncooperative Target.* MS thesis, AFIT/GAI/ENY/03-2. Graduate School of Engineering and Management, Air Force Institute of Technology (AU), Wright-Patterson Air Force Base OH, March 2003.

Grossman, Elaine M. and Keith J. Costa. "Small, Experimental Satellite May Offer More Than Meets The Eye," *Inside the Pentagon*, 1 (4 December 2003a). 4 December 2003 http://ebird.afis.osd.mil/ebfiles/s20031204238454.html.

-----. "USAF Leaders Identify Gaps In Ability To Interpret Space Events," *Defense Information and Electronic Report*, 1 (26 September 2003b).

Johnson-Freese, Joan. "The Viability of U.S. Anti-Satellite (ASAT) Policy: Moving Toward Space Control," INSS Occasional Paper 30, Space Policy Series, January 2000.

Levis, Alexander H. Class handout, SENG 640, Systems Architectures. Graduate School and Engineering and Management, Air Force Institute of Technology, Wright-Patterson AFB OH, January 2003.

Morring, Frank Jr. "Smallsats Grow up," *Aviation Week & Space Technology*, 46 (8 December 2003).

Murry, C. and Cox, C.B. *Apollo: The Race to the Moon.* New York: Simon & Schuster, 1989.

"One Year in Orbit for First DMC Satellite – AISAT-1," Surrey Satellite Technology Ltd. website. 1 February 2004 http://www.sstl.co.uk/index.php?loc=6.

Partch, Russell E., Vern Baker, and Clark Keith. "Autonomous Proximity Satellites," *Air Force Research Laboratory, Technology Horizons: Research for America's Future,* 4: 16-18 (December 2003).

"SAINT," Encyclopedia Astronautica website, (26 November 2003). 7 February 2004 http://www.astronautix.com/craft/saint.html.

Tragesser, Steven G. Class handouts, MECH 532, Introduction to Space Flight Mechanics; MECH 533, Intermediate Space Flight Dynamics. Graduate School of Engineering and Management, Air Force Institute of Technology, Wright-Patterson AFB OH, January 2003.

Tschirhart, Troy A. *A Study of Control Laws for Microsatellite Rendezvous with a Noncooperative Target.* MS Thesis, AFIT/GAI/ENY/03-3. Graduate School of Engineering and Management, Air Force Institute of Technology (AU), Wright-Patterson Air Force Base OH, March 2003.

Wertz, James R. and Wiley J. Larson. *Space Mission Analysis and Design (3rd Edition).* El Segundo CA: Microcosm Press, 1999.

Wieringa, R.J. "Combining static and dynamic modeling methods: A comparison of four methods," *The Computer Journal,* 38(1), 17-30 (1995).

Wiesel, William E. *Modern Orbit Determination (Prepublication Edition).* 2003.

-----. *Spaceflight Dynamics (2nd Edition)*. Boston MA: Irwin McGraw-Hill, 1997.

Wilson, J.R. "The Ultimate High Ground," *Armed Forces Journal*, 28 (January 2004). 8 January 2004 http://ebird.afis.osd.mil/ebfiles/s20040107246884.html.

XSS-10 Microsatellite Fact Sheet, Air Force Research Laboratory, Kirtland AFB NM. 18 November 2001 http://www.vs.afrl.af.mil/Factsheets/XSS10.html.

REPORT DOCUMENTATION PAGE

Form Approved
OMB No. 074-0188

1. REPORT DATE *(DD-MM-YYYY)*	2. REPORT TYPE	3. DATES COVERED *(From – To)*
23-03-2004	Master's Thesis	June 2003 – March 2004

4. TITLE AND SUBTITLE

SYSTEMS-LEVEL FEASIBILITY ANALYSIS OF A MICROSATELLITE RENDEZVOUS WITH NON-COOPERATIVE TARGETS

5a. CONTRACT NUMBER

5b. GRANT NUMBER

5c. PROGRAM ELEMENT NUMBER

6. AUTHOR(S)

Toso, Allen R., Major, USAF

5d. PROJECT NUMBER
2003-058

5e. TASK NUMBER

5f. WORK UNIT NUMBER

7. PERFORMING ORGANIZATION NAMES(S) AND ADDRESS(S)
Air Force Institute of Technology
Graduate School of Engineering and Management (AFIT/EN)
2950 Hobson Way, Building 640
WPAFB OH 45433-8865

8. PERFORMING ORGANIZATION REPORT NUMBER
AFIT/GSS/ENY/04-M06

9. SPONSORING/MONITORING AGENCY NAME(S) AND ADDRESS(ES)

10. SPONSOR/MONITOR'S ACRONYM(S)

11. SPONSOR/MONITOR'S REPORT NUMBER(S)

12. DISTRIBUTION/AVAILABILITY STATEMENT

APPROVED FOR PUBLIC RELEASE; DISTRIBUTION UNLIMITED.

13. SUPPLEMENTARY NOTES

14. ABSTRACT

The feasibility of using a microsatellite to accomplish an orbital rendezvous with a noncooperative target was evaluated. This study focused on identifying and further exploring the technical challenges involved in achieving a noncooperative rendezvous. A system engineering analysis and review of past research quickly led to a concentration on the guidance, navigation, and control elements of the microsatellite operation. The integration of control and orbit determination algorithms was investigated. A simple yet robust solution could not be found to meet reasonable rendezvous criteria, using essentially off-the-shelf technology and algorithms. System feasibility has been assessed to have a low probability in the very near term.

15. SUBJECT TERMS
Control, Estimation, Guidance, Microsatellite, Navigation, Rendezvous, Spacecraft

16. SECURITY CLASSIFICATION OF:			17. LIMITATION OF ABSTRACT	18. NUMBER OF PAGES	19a. NAME OF RESPONSIBLE PERSON
a. REPORT	b. ABSTRACT	c. THIS PAGE			Dr. Steven G. Tragesser
U	U	U	UU	115	19b. TELEPHONE NUMBER *(Include area code)* (937) 255-6565, ext 4286 (steven.tragesser@afit.edu)

Standard Form 298 (Rev. 8-98)
Prescribed by ANSI Std. Z39-18